

Semi-empirical Models of Galaxy Formation and Evolution

Andrea Lapi^{a,b,c,d}, Lumen Boco^{a,b,e} and Francesco Shankar^f

^aScuola Internazionale Superiore Studi Avanzati (SISSA), Physics Area, Via Bonomea 265, 34136 Trieste, Italy

^bInstitute for Fundamental Physics of the Universe (IFPU), Via Beirut 2, 34014 Trieste

^cIstituto Nazionale Fisica Nucleare (INFN), Sezione di Trieste, Via Valerio 2, 34127 Trieste, Italy

^dIstituto di Radio-Astronomia (IRA-INAF), Via Gobetti 101, 40129 Bologna, Italy

^eInstitut für Theoretische Astrophysik, ZAH, Universität Heidelberg, Albert-Ueberle-Str. 3, 69120 Heidelberg, Germany

^fSchool of Physics and Astronomy, University of Southampton, Highfield, Southampton, SO17 1BJ, UK

© 20xx Elsevier Ltd. All rights reserved.

Chapter Article

Glossary

Galaxies gravitationally bound ensembles of stars, gas and dust found throughout the universe.

Dark matter putative non-luminous matter interacting with the ordinary one (e.g., atoms) solely via gravitational forces.

Black holes celestial objects featuring a gravitational field so strong that even light cannot escape it.

Nomenclature

DM	Dark Matter
SIMs	(Hydrodynamical) Simulations
SAMs	Semi Analytic Models
SEM	Semi Empirical Models
SMHM	Stellar Mass Halo Mass (Relationship)
(s)SFR	(Specific) Star Formation Rate
(s)HAR	(Specific) Halo Accretion Rate
BHs	Black Holes

Abstract

We provide a review on semi-empirical models of galaxy formation and evolution. In Section 1 we present a brief census of the three main modeling approaches to galaxy evolution, namely hydrodynamical simulations, semi-analytic models, and semi-empirical models (SEMs). In Section 2 we focus on SEMs in their different flavors, i.e. interpretative, descriptive and hybrid, discussing the peculiarities and highlighting virtues and shortcomings for each of these variants. In Section 3 we dissect a simple and recent hybrid SEM from our team to highlight some technical aspects. In Section 4 we offer some outlook on the prospective developments of SEMs. In Section 5 we provide a short summary of this review.

Key points

- Semi empirical models (SEM) are effective, data-driven, easily expandable and computationally low-cost approaches to galaxy evolution, complementary to (semi-)analytic models and numerical simulations.
- Descriptive SEMs produce realistic snapshots of the Universe at a given cosmic time. Interpretative SEMs serve to test specific hypotheses or consistency among different datasets. Hybrid SEMs feature elements partly in line with an interpretative and partly with a descriptive viewpoint.
- SEMs are being exploited to address open issues in galaxy evolution like galaxy quenching mechanisms and the coevolution of galaxies and supermassive black holes. A strong synergy of SEMs with data science techniques could also be foreseen in the near future.

1 Introduction: the triumvirate of galaxy formation models (SIMs, SAMs, and SEMs)

Acquiring a comprehensive picture for the formation and evolution of galaxies in a cosmological context is one of the main challenges in modern astrophysics (see Mo et al. 2010; Silk and Mamon 2012; Maiolino and Mannucci 2019; Cimatti et al. 2020). Whilst a well-defined standard model exists in particle physics, there is no equivalent in the realm of extragalactic astrophysics, where major unknowns still limit our understanding of galaxy formation and evolution. Leading theories suggest that galaxies form from the condensation and cooling of pristine gas within virialized dark matter (DM) structures called halos. Ironically, the evolution of such an ‘obscure’ DM component is somewhat simpler and better understood than the ‘luminous’ baryonic one, since allegedly the only force at play among DM particles is (Newtonian) gravity. Cosmological N -body simulations have been able to precisely delineate the formation and evolution of DM halos and to extensively characterize their statistical properties. In contrast, the physics regulating baryons is intrinsically complex, since it involves many physical processes occurring on vastly different spatial, time, and energy scales.

2 Semi-empirical models

For example, it is well established that DM structures are formed in a hierarchical way, with larger halos gradually growing via the merging of smaller ones and/or mass accretion along filamentary structures of the cosmic web (e.g., Springel et al. 2006; Shandarin et al. 2012; Vogelsberger et al. 2014; Libeskind et al. 2018; Martizzi et al. 2019; Wilding et al. 2021; see also Angulo and Hahn 2022). However, observations suggest that star formation and stellar mass assembly in galaxies may follow an opposite, downsizing trend: massive galaxies form a significant part of their stellar mass earlier and rapidly, via a burst of intense star formation lasting less than a Gyr, while smaller ones form later on, over longer timescales of several Gyrs (see, e.g., Cowie et al. 1996; Thomas et al. 2005, 2010; Martín-Navarro et al. 2018; Merlin et al. 2019; Nanayakkara et al. 2022; Lah et al. 2023). Explaining these contrasting trends is particularly challenging for current models, which tend to accurately predict the properties of local galaxies, but struggle somewhat in understanding the strong star formation episodes and large stellar masses observed at high redshift (see Fontanot et al. 2007; Somerville et al. 2012, 2015; Hirschmann et al. 2016; Bassini et al. 2020; Lovell et al. 2021; Hayward et al. 2021; Lustig et al. 2023; Dome et al. 2024), unless specific assumptions are invoked such as a non-universal initial mass function (see Baugh et al. 2005; Lacey et al. 2016; Fontanot et al. 2017; Lapi et al. 2024b; Jeong et al. 2024), reduced effects of dust attenuation (e.g., Ferrara et al. 2023, 2024), alternative cosmologies (e.g., Menci et al. 2020, 2024) or modified gravity theories (e.g., McGaugh et al. 2024).

Another example of an important and mysterious issue in galaxy evolution concerns not the birth of galaxies, but rather their *deaths*. How do galaxies quench their star formation? Crucial hints for understanding star formation activity come from its relationship with galaxy morphology. In fact, up to very early epochs, on average it has been observed an intriguing correlation between star formation and morphology: elliptical galaxies or disk galaxies with a prominent bulge component are typically characterized by very low SFRs, while galaxies with a larger disk component tend to be star-forming (e.g., Wuyts et al. 2011; Dimauro et al. 2022; Driver et al. 2022). Nevertheless, as of now, there is no definitive observational evidence pinpointing the leading mechanism responsible for quenching galaxies: is it the presence of the stellar bulge itself that acts as the key driver behind quenching (e.g., Cook et al. 2009; Martig et al. 2009; Gensior et al. 2020)? Or instead morphological evolution and star formation activity are indirectly connected by some other physical phenomenon able to quench the galaxy and at the same time shape its morphology? In this context, could quenching be caused by the energy/momentum feedback from the supermassive black hole residing at the centre of galactic bulges (e.g., Silk and Rees 1998; Fabian 1999; Granato et al. 2004; Lapi et al. 2006; King 2005; King and Pounds 2015; Grand et al. 2017; Lapi et al. 2018; Valentini et al. 2020; Goubert et al. 2024)? Or even just by the host halo mass surpassing a certain threshold and causing the retention of a hot atmosphere screening the galaxy from external gas inflows (e.g., Birnboim and Dekel 2003; Kereš et al. 2005; Dekel and Birnboim 2006; Dekel et al. 2009, 2023)?

In the last three decades, the numerous facets of such open, complex problems have been investigated mainly via three ab-initio modeling approaches: hydrodynamical simulations (for a review, see Naab and Ostriker 2017), semi-analytic models (for a review, see Somerville and Davé 2015), and analytic frameworks (for a review, see Matteucci 2012). *Hydrodynamical simulations* (SIMs) allow to address the galaxy formation process in fine detail, as they can cope with the simultaneous evolution of DM, gas and stars. However, despite the recent increase in resolution and speed (mainly thanks to emulators and ‘genetic’ codes), many of the relevant physical processes still constitute sub-grid physics, while a detailed exploration of the parameter space is often limited by rather long computational times. Early SIMs struggled in forming cold, thin, and extended stellar disks, due to the overcooling of low-angular momentum baryons at high redshifts (see Katz and Gunn 1991; Navarro and Steinmetz 2000; Abadi et al. 2003). SIMs incorporating gas outflows related to stellar feedback mitigated the issue by preventing early cooling (see Scannapieco et al. 2008; Governato et al. 2010; Brook et al. 2011), and delaying the star formation history toward the present (see Brook et al. 2012; Stinson et al. 2013), though at the price of yielding outcomes that are sensitively dependent on the sub-grid recipes and the numerical treatment of the feedback itself (e.g., Scannapieco et al. 2012; Donnari et al. 2021; Habouzit et al. 2022; Crain and van de Voort 2023). Subsequent developments have focused on reproducing the overall galaxy structure, the metal abundance gradients, and the scaling relations among the integrated properties of local disk galaxies (see Guedes et al. 2011; Aumer et al. 2013; Vogelsberger et al. 2014; Hopkins et al. 2014; Crain et al. 2015; Schaye et al. 2015; Colín et al. 2016; Ceverino et al. 2017; Pillepich et al. 2018; Hopkins et al. 2018; Davé et al. 2019). Achieving these goals has required the introduction of educated star formation thresholds, and the setting of the feedback efficiency to high values. The latter has been considered also in possible connection with the activity of a central supermassive black hole (see De Lucia et al. 2006; Grand et al. 2017; Valentini et al. 2020; Wellons et al. 2023). The most recent SIMs are starting to fully address the detailed spatial and kinematical structure of galaxies and their cycle of multiphase gas across cosmic times (see Grand et al. 2019; Pillepich et al. 2019; Vincenzo et al. 2019; Buck et al. 2020; Pandya et al. 2021; Feldmann et al. 2023).

Semi-analytic models (SAMs) are based on DM merger trees extracted from N -body simulations (or generated via Monte Carlo procedures gauged on them), while the physics inside dark halos is modeled via parametric expressions set on (mainly) local observables. These models are less computationally expensive than hydro simulations and enable to more clearly disentangle the relative role of the diverse physical processes, though the considerable number of fudge parameters describing the underlying physics can lead to degenerate solutions and restrict somewhat the predictive power, especially toward high redshift. Early attempts based on simple recipes for cooling and stellar feedback from supernova explosions yielded encouraging results in reproducing the properties of local disk galaxies such as sizes, scaling relations, and statistics (see Kauffmann et al. 1993; Lacey and Cole 1993; Cole et al. 2000; Baugh et al. 2005). Through the years, these basic prescriptions have been progressively refined to describe additional processes and further improve the agreement with observations, even toward high redshifts. Specifically, modern SAMs incorporate energy feedback from accreting supermassive black holes (see Croton et al. 2006; Monaco et al. 2007; Somerville et al. 2008; Benson 2012; Fontanot et al. 2020), merger-driven bursts of star formation and dust

absorption/emission effects (see Baugh et al. 2005; Cook et al. 2009; Lacey et al. 2016), recycling of blown-out gas via galactic fountains (see Henriques et al. 2015; Croton et al. 2016), metal enrichment in gas and stars (see Cousin et al. 2016; Hirschmann et al. 2016), multi-phase treatment of atomic and molecular gas components (see Somerville et al. 2015; Lagos et al. 2018; Baugh et al. 2019), radial structure and gradients (see Stevens et al. 2016; Henriques et al. 2020) and related transport processes of gas and stars (see Forbes et al. 2019), and the effects of DM halo growth rate, gas fraction and angular momentum increase/dissipation on the emergence of galaxy properties (see Cook et al. 2009; Cattaneo et al. 2017; Barrera et al. 2023; Mo et al. 2023).

It is also worth mentioning the role of frameworks that admit fully analytic solutions. They are necessarily based on approximate and spatially/time-averaged descriptions of the most relevant astrophysical processes; however, their transparent, handy, and predictive character often pays off on some specific issues. Pioneering works were focused on the chemical evolution of the Milky Way, and highlighted the relevance of gas inflow and outflow processes in reproducing the metal abundance of the solar neighborhood (see Schmidt 1963; Talbot and Arnett 1971; Tinsley 1974; Pagel and Patchett 1975; Hartwick 1976; Chiosi 1980; Matteucci and Greggio 1986; Edmunds 1990). Successive developments concerned the mechanisms leading to dust production (see Dwek 1998; Hirashita 2000; Inoue 2003; Zhukovska et al. 2008), the abundance gradients in the Galactic disk (see Chiappini et al. 2001; Naab and Ostriker 2006; Grisoni et al. 2018), steady-state equilibrium models among star formation, inflows and outflows (see Bouché et al. 2010; Davé et al. 2012; Lilly et al. 2013; Pipino et al. 2014; Feldmann 2015; Pantoni et al. 2019; Lapi et al. 2020), effects of the initial mass function and of stellar yield models (see Mollá et al. 2015; Recchi et al. 2015), differential and/or selective winds (see Recchi et al. 2008), dichotomy among active and passive galaxies (see Spitoni et al. 2017), and detailed inside-out growth of galaxy disks with radial mixing (see Andrews et al. 2017; Frankel et al. 2019).

All in all, it is fair to state that in relation to the aforementioned open problems about downsizing, quenching and galaxy morphological evolution, all these ab-initio theoretical approaches somewhat struggle in highlighting the primary physical mechanism responsible for them. They offer insights into the influence of the diverse physical processes, yet their outcomes are contingent on the chosen physical models, sub-grid recipes and resolution (see Scannapieco et al. 2012; Donnari et al. 2021; Crain and van de Voort 2023). To partly bypass these shortcomings, a complementary approach to probe galaxy evolution has emerged, namely the so-called *semi-empirical models* (SEMs) as pioneered by different research groups (e.g., Hopkins et al. 2006; Hopkins and Hernquist 2009; Moster et al. 2013, 2018; Behroozi et al. 2013, 2019, 2020; Shankar et al. 2014; Mancuso et al. 2016a,b, 2017; Buchan and Shankar 2016; Grylls et al. 2019; Hearin et al. 2022; Drakos et al. 2022; Fu et al. 2022, 2024; Boco et al. 2023; Zhang et al. 2023, 2024a). SEMs adopt an ‘effective’ approach to galaxy evolution: they do not attempt to model the small-scale physics regulating the baryon cycle from first principles, but marginalize over it by exploiting empirical relations between the spatially-averaged properties of galaxies (e.g., stellar mass, SFR, specific SFR) and DM halos (e.g., halo mass, accretion rate, or circular velocity), derived from their relative abundance or from analytic parameterizations. The value of these models stands in that they feature by design a minimal set of assumptions and parameters gauged on observations. By focusing just a few aspects they allow to transparently investigate specific and still unclear/debated aspects of galaxy formation and evolution, in a bottom up fashion. Moreover, by empirically linking different observables, they can test for possible inconsistencies among distinct datasets, which can often occur given the significant observational systematics. Finally, these frameworks are particularly helpful when galaxy formation recipes must be coupled with those from other branches of astrophysics (e.g. stellar evolution, planetary science, radiative transfer codes, etc.), and therefore it is worth to minimize the uncertainties/hypotheses at least on the former side by exploiting basic data-driven inputs (e.g., Lapi et al. 2024a; Roy and Lapi 2024). However, semi-empirical models are not free of downsides. By construction they strongly rely on data and, therefore, it is essential to input them with robust determinations of galaxy statistics and scaling relations between baryonic and halo properties to build a successful framework.

2 SEMs in their different flavors: descriptive, interpretative, hybrid

The basic setup of a SEM requires to establish a connection between the properties of DM halos and galaxies. Specifically, starting from a DM halo statistics and/or catalog extracted from a N -body simulation, SEMs populate the halos with galaxies via matching the statistical distributions of two different physical quantities, one related to DM and the other to the baryonic component. Such an ‘abundance matching’ technique implicitly assumes the existence of a monotonic relationship between two quantities, X and Y , one related to halos and one to baryons, and matches their cumulative statistical distributions $P(> X)$ and $P(> Y)$. For example, on the DM side X can be the halo mass M_H and $P(> M_H)$ can be easily constructed from the halo mass function $N(M_H, z)$ extracted from N -body simulations. On the baryonic side Y can be the stellar mass M_* and $P(> M_*)$ can be built from the observed galaxy stellar mass function $N(M_*, z)$. The main problem of such an abundance matching technique is that perfect monotonic relations do not always efficiently capture all the physics involved: galaxies and halos will often feature a certain distribution in the $X - Y$ plane, spread out by the degeneracies with many other nuisance parameters. However, abundance matching techniques do not allow to derive such a full distribution, but just an average relation $Y(X)$ and, even when scatter is kept into account, it is often assumed Gaussian and guessed a priori (see Aversa et al. 2015). For this reason, every SEM based on abundance matching requires an assumption of monotonicity between two quantities and a free parameter, namely the scatter on their relation. Nevertheless, abundance matching constitutes a powerful tool to understand how different observables relate to each other, and to address systematic uncertainties in the statistical distributions from which the cumulative probabilities are built (especially the baryonic related ones).

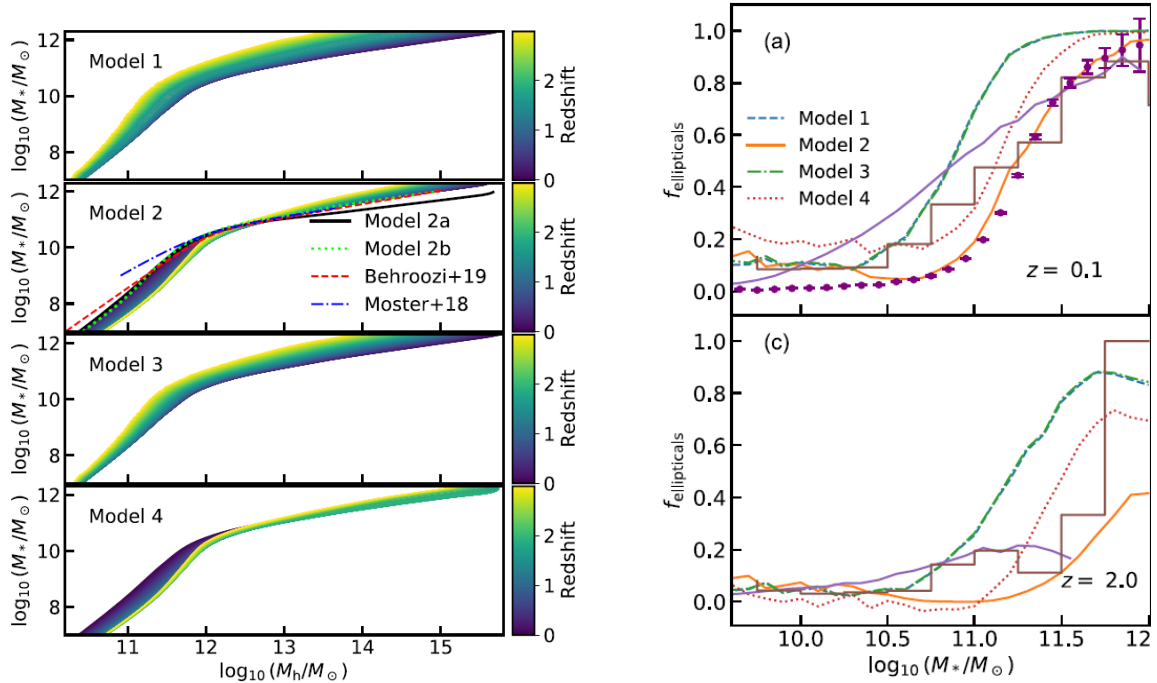


Fig. 1 Figures from Fu et al. (2022) highlighting some results of the DECODE model. The left panel illustrates the SMHM relationship at different redshift (color-coded) computed via abundance matching of the halo mass and stellar mass functions. The four panels refer to different models for the shape and evolution of the stellar mass function; in the second from the top, the local relations from the EMERGE (dot-dashed line) and UNIVERSEMACHINE (dotted line) SEMs are reported. The right panel illustrates the fraction of elliptical galaxies vs. the stellar mass at two representative redshifts $z \approx 0.1$ (top panel) and $z \approx 2$ (bottom panel), for the same four models. Data from the SDSS survey (magenta circles), the GALICS SAM (solid magenta line; see Koutsouridou and Cattaneo 2022) and the TNG100 SIM (magenta histogram; see Nelson et al. 2019) are reported.

The very first attempts to link galaxies and host halos via abundance matching involved the luminosity and halo mass (e.g., Vale and Ostriker 2004, 2006; Shankar et al. 2006). Through the years, the most commonly employed relation has been the one between the halo mass M_H and stellar masses M_* , called stellar mass-halo mass (SMHM) relation (e.g., Hopkins and Hernquist 2009; Conroy and Wechsler 2009; Behroozi et al. 2010; Moster et al. 2010; Yang et al. 2012; Zavala et al. 2012; Behroozi et al. 2013; Moster et al. 2013; Shankar et al. 2014; Rodríguez-Puebla et al. 2017; Tollet et al. 2017; Grylls et al. 2019; Fu et al. 2022). More recently, people have started using more sophisticated, additional mappings between the time derivative of the masses (e.g., Fu et al. 2024), i.e. the star formation rate \dot{M}_* vs. the halo accretion rate \dot{M}_H , or even between the specific rates (see Boco et al. 2023), i.e. the specific SFR \dot{M}_*/M_* and the specific halo accretion rate \dot{M}_H/M_H . A recent example of a SEM following the aforementioned foundational framework is constituted by the DECODE model (see Fu et al. 2022), where abundance matching techniques are exploited to derive the SMHM relation and the merger histories of central and satellite galaxies. Specifically, the main focus is to highlight the dependence of these derived quantities on the observational determination of the stellar mass function up to the cosmic noon at redshift $z \sim 2$. A few outcomes of DECODE can be found in Figure 1; these showcase that when different renditions of the local stellar mass function and of its redshift evolution are adopted, the SMHM relation and the fraction of elliptical galaxies change accordingly (at fixed theoretical assumptions, e.g. role of major mergers in their formation path). Remarkably, it turns out that only SMHM relations derived from stellar mass functions featuring large number densities of massive galaxies and significant redshift evolution (‘Model 2’ in the Figure) can simultaneously reproduce the local abundances of satellite galaxies, the major merger statistics as inferred from galaxy pairs, and the local fraction of elliptical galaxies. This is an example of how a SEM can be exploited to have a handle on possible systematic uncertainties in the observational determination of a statistical distribution like the stellar mass function. For this reason, SEMs with this flavor may be referred to as *interpretative*.

An alternative SEM framework envisages to connect DM halo and galaxy properties by assuming a parametric form of an empirical relation expected between two quantities (inspired from observational evidence or theoretical arguments), and by fitting such parameters by comparison with other independent observables. An example could be to parameterize the local SMHM relation in terms of a double power-law behavior $M_*(M_H, z) = \epsilon M_H / [(M_H/M_c)^\alpha + (M_H/M_c)^\beta]$, with ϵ a normalization, M_c a characteristic mass, α and β two slopes at large and small halo masses. Furthermore, the redshift evolution of the relation may in turn be rendered via a polynomial dependence of the above quantities in terms of the scale factor $a \equiv 1/(1+z)$, e.g. $\epsilon = \epsilon_0 + \epsilon_z(1-a)$ with ϵ_0 and ϵ_z the fitting parameters. Plainly, the complexity of such a description depends on the number of parameters and quantities designed to be fitted (e.g., Moster et al. 2018; Behroozi et al. 2019;

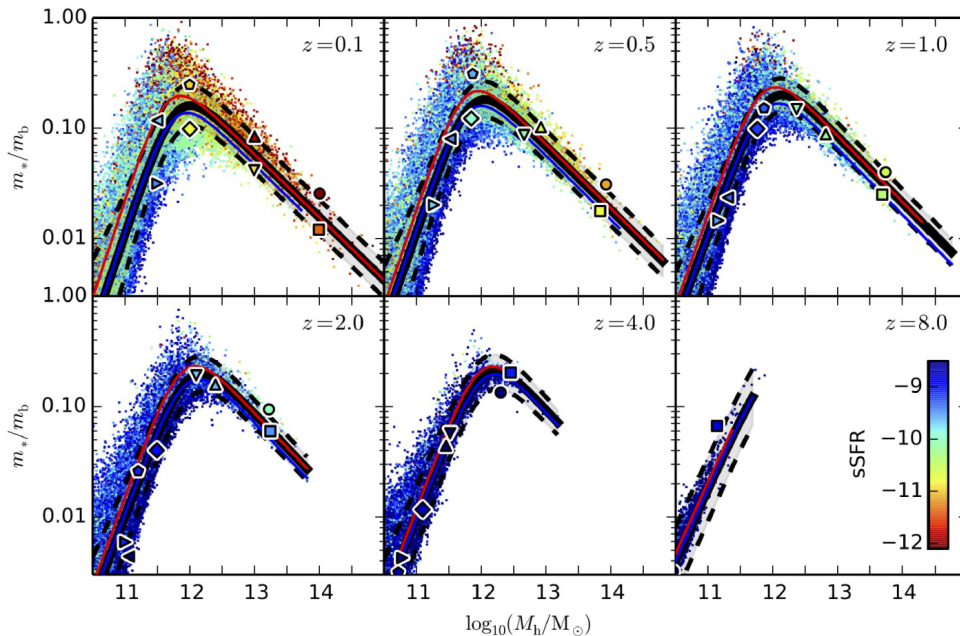


Fig. 2 Figure from Moster et al. (2018) illustrating the redshift-dependent SMHM derived from EMERGE at different redshifts from $z \approx 0.1$ to $z \approx 8$ (from top left to bottom right), expressed in terms of the integrated conversion efficiency $M_*/0.16 M_H$ vs. the halo mass M_H . Color-code refers to the logarithm of the specific SFR $\log \dot{M}_*/M_*$ in units of yr^{-1} . Solid black lines show the median and the dashed black lines show the 1σ scatter. The red and blue solid lines are the median for quenched and starforming galaxies. The large symbols in each panel represent eight individual systems that have been selected from the upper and lower 1σ contours for four halo masses at $z \approx 0.1$, and traced back in cosmic time.

Grylls et al. 2020). A specific example of this approach is constituted by EMERGE (Empirical Model for the formation of GalaxiEs; see Moster et al. 2018). It assigns galaxies to DM halos by parameterizing a redshift-dependent SFR vs. halo accretion rate relation, and then fit for the parameters exploiting the observational constraints on stellar mass function, cosmic SFR density and quenched galaxy fractions. The added value of this approach is that the SMHM relation and its scatter, together with the associated redshift evolution, comes out as predictions of the model (see Figure 2). Another example worth mentioning is UNIVERSEMACHINE (see Behroozi et al. 2019). This SEM assumes a parameterized relation between the SFR and the peak circular velocity (related to the maximum mass attained over the halo’s assembly history) which, along with quenched galaxy fractions, is used to assign a SFR probability distribution to each DM halo. These distributions are exploited to compute individual SFRs for halos and then the latter quantity is integrated in time to derive galaxy stellar mass growth tracks. The galaxy stellar mass function, cosmic SFR, correlation functions and other quantities are predicted as outputs of the model. In a subsequent, very interesting development (see Behroozi et al. 2020), UNIVERSEMACHINE has been also exploited to generate mock galaxy catalogs and light-cones over an extended redshift range up to $z \sim 15$, providing specific predictions for JWST surveys to be confronted with recent and upcoming data (see Figure 3). SEMs like the two above are designed with many parameters to be fitted, and are closer in this respect to a full-fledged SAM. However, they still keep a close link between parameters and observations typical of the SEM spirit, and allow to choose an educated, empirical parameterization not necessarily anchored to an ab-initio theoretical modeling of the physical processes at play. This approach has the added value of easing the removal of degeneracies among parameters, the exploration of the full parameter space, and the optimization of parameters via standard model selection statistics. SEMs with this flavor may be referred to as *descriptive*.

Finally, other frameworks try to complement the basic setup of a descriptive SEM on some galaxy properties, with the integration of interpretative elements to constrain some underlying physical processes. Like any other SEMs, such approaches are expressly designed to rely on a limited set of assumptions and parameters, rendering the model almost fully data-driven. But then specific physical hypotheses are applied on top of this basic scheme and each of the putative triggers for a phenomenon is systematically tested, in isolation or in combination with others, against the observed abundances and properties of galaxies at different cosmic epochs. Such an approach is different from a descriptive SEM, because it goes beyond establishing relationships between various properties of halos and galaxies. Instead, it aims to elucidate how different theoretical hypotheses on a phenomenon may influence these relationships. The effect of adding, removing, or changing such a physical hypothesis for a phenomenon will manifest visibly in the outputs and can be directly compared to observational data. Such kind of SEMs may be helpful to address the longstanding issues in galaxy evolution recalled in Section 1. For example, the effectiveness of such novel approaches has been recently demonstrated in the TOPSEM model (Two Parameter Semi-Empirical Model; see Boco et al. 2023), which is capable of reproducing the galaxy morphology with a minimal set of assumptions and parameters. Specifically, after constructing a mock catalog of galaxies via abundance matching, TOPSEM tests a theoretical hypothesis for the morphological evolution

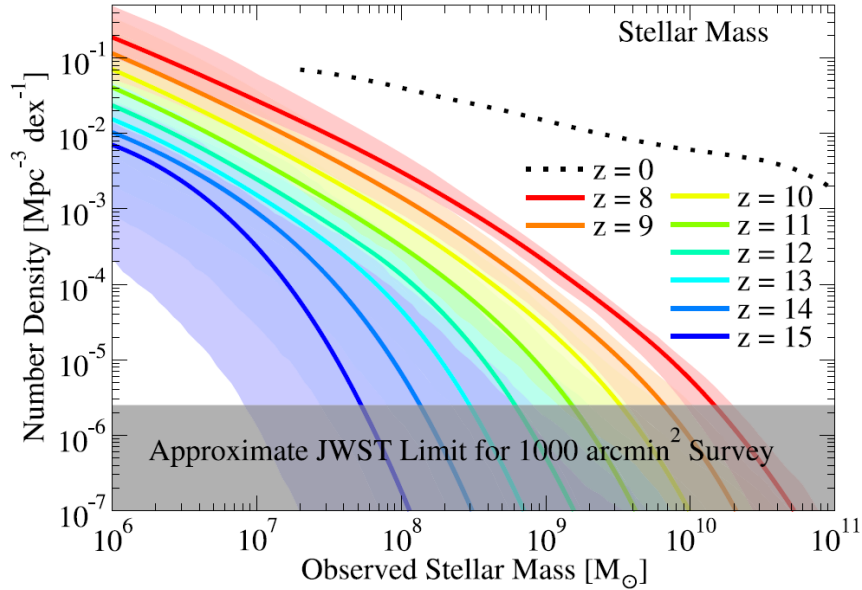


Fig. 3 Figure from Behroozi et al. (2020) highlighting predictions of UNIVERSEMACHINE for the stellar mass function at high redshift from $z \approx 8$ to $z \approx 15$ (color-coded), in terms of median values (solid lines) and 1σ confidence intervals (colored areas). The local stellar mass function is also reported as a dotted black line. The approximate limit of a JWST survey over 1000 arcmin^2 is displayed as a grey shaded area.

of galaxies, strictly linking it to the host DM halo growth (see next Section for details). Physical scenarios for quenching and downsizing are also starting to be investigated with this kind of approach (e.g., Fu et al. 2025; see Section 4). All in all, such a way of testing physical hypotheses on top of empirical frameworks embodies partly interpretative and partly descriptive components, and for this reason this type of SEM may be referred to as *hybrid*.

3 Dissecting a hybrid SEM

In this Section we present some details of a recent model from our research team, dubbed TOPSEM: Two-Parameters Semi Empirical Model (see Boco et al. 2023), as an example of the very simple and effective approach typical of a SEM. We will show that on the one hand this straightforward model is able to reproduce crucial aspects of galaxy evolution, such as the stellar mass assembly in galaxies, and on the other hand it can be exploited to test specific hypotheses on the origin of galaxy morphology, so addressing some of the pressing issues recalled in Section 1. TOPSEM relies on one main assumption, one boundary condition, and two parameters associated to them. The assumption is about a monotonic correlation between galaxies' specific star formation rate (sSFR) and specific halo accretion rate (sHAR), with sSFR being the ratio between star formation rate and stellar mass of a galaxy and sHAR being the ratio between halo accretion rate and halo mass. This assumption means that galaxies with larger sSFR reside in halos with larger sHAR. The model relies on abundance matching of these specific rates to derive the sSFR-sHAR relationship. Building on that, DM halos are populated with galaxies of given SFR and stellar masses, effectively constructing a mock catalog of galaxies equipped with their own stellar mass assembly history.

Such a mock catalog is used to test a theoretical hypothesis on the morphological evolution of galaxies, in the spirit of the hybrid SEMs described in the previous Section. This hypothesis is based on a two-phase galaxy evolution scenario, where the formation of bulges and disks is linked to the two-mode DM halo accretion histories. Specifically, N -body simulations analyses (e.g., Wechsler et al. 2002; Zhao et al. 2003, 2009; Diemand et al. 2007; Hoffman et al. 2007; Ascasibar and Gottlöber 2008; More et al. 2015; Hearin et al. 2021) have highlighted that mass accretion history of halos can be roughly divided into two distinct phases: an early fast accretion phase dominated by major mergers and violent collapse, which shapes the structure of the inner halo potential well, and a later slow accretion phase characterized by a smoother DM accretion or minor mergers and usually dominated by 'pseudo-evolution' (Diemand et al. 2007; Diemer et al. 2013; Zemp 2014; More et al. 2015), which contributes to growing the halo outskirts though not altering the central structure. The hypothesis tested is that bulges and spheroidal components are formed during the early fast accretion phase, when violent accretion processes and dynamical friction between giant gas clumps leads to a quick loss of angular momentum also for baryonic matter that rapidly sinks to the very central region and triggers violent star formation episodes (e.g., Lapi et al. 2018; Pantoni et al. 2019). Galactic stellar disks are instead formed during the later slow accretion phase when baryons can retain part of their angular momentum and are not directly funneled toward

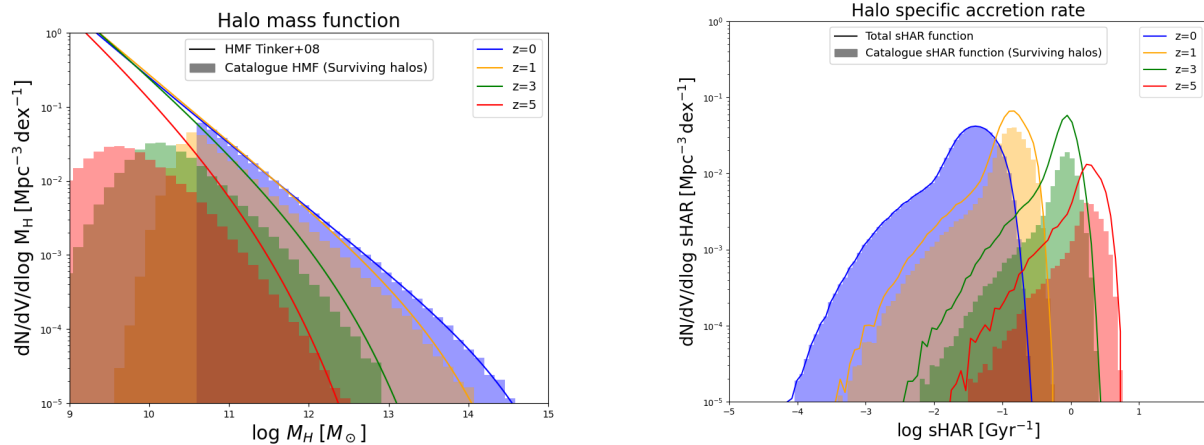


Fig. 4 Figure from Boco et al. (2023) showing the halo mass function (left panel) and sHAR function (right panel) at different redshifts: blue $z = 0$, orange $z = 1$, green $z = 3$, and red $z = 5$. Histograms are the distributions for a mock catalog of surviving halos, whereas solid lines refer to the reconstructed total distribution for all the halos.

the center. Such an idea builds upon the pioneering works of Mo and Mao (2004) and Cook et al. (2009) and can qualitatively explain stellar archaeological results showing stellar population of bulges/spheroids to be older, α -enhanced and rapidly generated, and stars in disks to be younger and formed over longer timescales (see, e.g., Cowie et al. 1996; Chiappini et al. 1997; Thomas et al. 2005, 2010; Gallazzi et al. 2006; Johansson et al. 2012; Courteau et al. 2014; Pezzulli and Fraternali 2016; Grisoni et al. 2017; Bellstedt et al. 2024; Mo et al. 2023). In TOPSEM the interplay between the transition time from fast to slow accretion and the quenching time would lead to the generation of different types of galaxies, from grand-design disks to pure ellipticals. As shown in section 3.3, the model naturally predicts the stellar mass function for bulges and ellipticals and the fraction of ellipticals, that are found to be in agreement with the observational determination from the GAMA survey by Moffett et al. (2016a,b).

3.1 Empirical relations for halos and galaxies

The first step for every SEM is to build a catalog of DM halos, which is then populated with galaxies by means of empirical relations. Halo statistics and their evolution are completely set by N -body simulation results. In TOPSEM a discrete halo catalog at $z = 0$ is built by sampling the halo mass function determination from Tinker et al. (2008), tracing the halo growth history backward in time using the DIFFMAH code from Hearin et al. (2021). The catalog constructed with this method naturally comprises and tracks the evolution of all the halos surviving at $z = 0$, but does not include the non-surviving halos, i.e., the ones which merge or are disrupted at higher redshift. The catalog is used to extract statistical distributions of meaningful halo properties, such as their mass and specific halo accretion rate, which are useful for building the model. Figure 4 shows the redshift evolution of the halo mass function (left panel) and of the sHAR function (right panel). Histograms refer to the halos in the catalog, while solid lines to the reconstructed distribution for all the halos at a given redshift, both surviving and non-surviving. In order to reconstruct the non-surviving halo distribution, it is assumed that each non-surviving halo of a given mass follows the same sHAR distribution as surviving halos of the same mass. This assumption is supported by the fact that, prior to becoming satellites of larger halos, non-surviving halos can be treated as centrals, exhibiting a sHAR distribution statistically similar to that of other halos with the same mass (see Boco et al. 2023 for details). In this way, the effect of non-surviving halos is accounted for in TOPSEM results. As expected, higher redshift halos tend to have smaller masses and higher specific accretion rates.

For the treatment of the complex baryonic component, TOPSEM relies on empirical quantities and relations at different redshifts, which provide a snapshot of galaxy properties at any cosmic time. These include the stellar mass function both for starforming and quiescent galaxies (e.g., Ilbert et al. 2013; Tomczak et al. 2014; Bernardi et al. 2017; Davidzon et al. 2017; Weaver et al. 2023), describing how stellar mass is distributed among galaxies, and the main sequence of starforming galaxies (e.g., Daddi et al. 2007; Rodighiero et al. 2011; Sargent et al. 2012; Béthermin et al. 2012; Rodighiero et al. 2015; Speagle et al. 2014; Whitaker et al. 2014; Ilbert et al. 2015; Schreiber et al. 2015; Mancuso et al. 2016a; Dunlop et al. 2017; Bisigello et al. 2018; Pantoni et al. 2019; Lapi et al. 2020; Popesso et al. 2023; Huang et al. 2023), a well-known correlation between stellar mass and SFR at given redshift. In particular, TOPSEM adopts the fits proposed by Davidzon et al. (2017) for the stellar mass function (left panel in Figure 5) and the main sequence determination by Popesso et al. (2023). By convolving stellar mass function and main sequence (see Boco et al. 2021a, 2023), TOPSEM derives the sSFR distributions competing to star-forming galaxies at any given cosmic epoch (right panel in Figure 5).

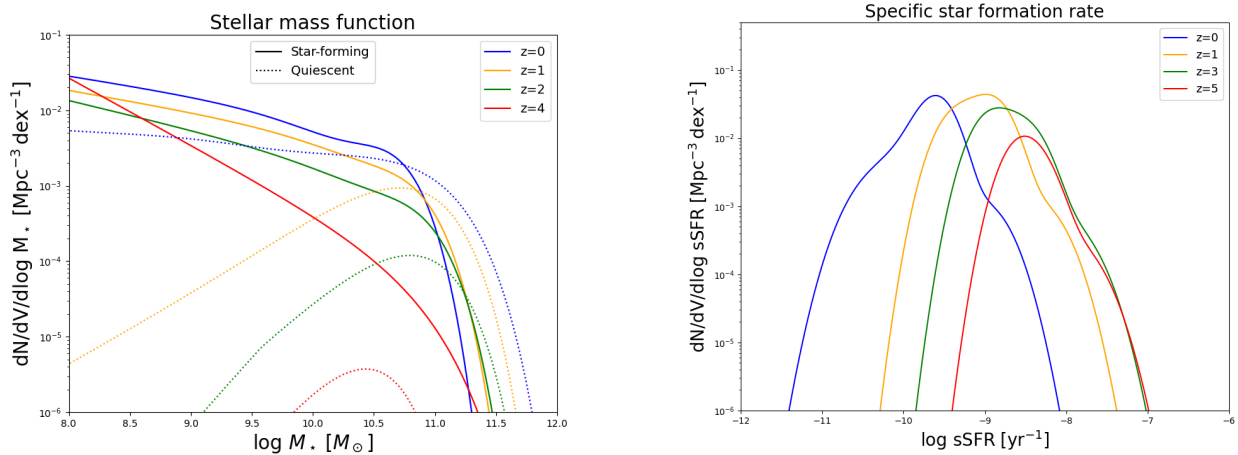


Fig. 5 Figure from Boco et al. (2023) showing the stellar mass function (left panel) from Davidzon et al. (2017) for star-forming (solid lines) and quiescent galaxies (dotted lines), and the sSFR distribution (right panel) from the convolution of the stellar mass function of active galaxies and the main sequence. Colors are as in Figure 4.

3.2 Populating halos with galaxies

In the previous Section we have described the main ingredients needed to construct a SEM: the results of N -body simulations for the halo accretion history, and empirical quantities such as the stellar mass function and the main sequence for the baryonic component. The aim of a SEM is to connect these two components in an empirical way. TOPSEM establishes this link via abundance matching between sSFR and sHAR, so innovating with respect to the standard abundance matching between stellar mass and halo mass. In fact, stellar and halo masses can depend on the history of mass accretion, while specific quantities better capture the situation at a given time. This is because the SFR of a galaxy is expected to be somewhat linked to the halo accretion rate, since a faster DM accretion would correspond to a faster gas inflow and, consequently, to more gas available to form stars. On top of that, star formation efficiency, the amount of baryons converted into stars, can heavily change for objects with different masses (e.g., Moster et al. 2010, 2013, 2018; Behroozi et al. 2013, 2019; Aversa et al. 2015; Rodríguez-Puebla et al. 2017), possibly creating some scatter around the mean SFR-HAR relation. To marginalize over this effect, TOPSEM performs abundance matching between two mixed quantities $\text{sSFR} = \psi/M_*$, and $\text{sHAR} = \dot{M}_H/M_H$, searching for a relation $\psi/M_* = f(\dot{M}_H/M_H)$ where $f(\cdot)$ is a monotonic function to be found. Therefore, the main assumption of the model is the monotonicity in the sSFR-sHAR relation and the first free parameter is the scatter $\sigma_{\log \text{sSFR}}$ around this relation. Before giving the details of the abundance matching procedure and the results, two important remarks are in order:

- sSFR alone is not useful to fully characterize a galaxy star formation history if the stellar mass at a certain time is not known (translating sSFR to SFR requires the knowledge of M_*). For this reason TOPSEM needs a boundary condition for the stellar masses of the mock galaxies. These are initialized at $z \approx 0$, since we dispose of more complete and robust observational data in the local Universe with respect to high redshift. Such initialization is done on the basis of the $z \approx 0$ SMHM relation (see Reyes et al. 2012; Mandelbaum et al. 2016; Lapi et al. 2018), and the related scatter $\sigma_{\log M_*}$ is the second parameter of the model. Then star formation histories of galaxies are followed backwards in time. Note that TOPSEM uses only the $z \approx 0$ SMHM as boundary condition, but the evolution of the relation is a prediction not an input.
- TOPSEM assumes that only star-forming galaxies follow the sSFR-sHAR relation, not quenched ones. Indeed, the sSFR function displayed in Figure 5 is valid only for star-forming galaxies; sSFR for quiescent ones are highly uncertain and rather disperse. Moreover, if the relation between sSFR and sHAR is applied to all the halos and galaxies, it would naturally provide an explanation for quenching related to the accretion history of the DM halo: quenched galaxies, having low sSFR, would be classified as the ones embedded in low sHAR halos. However, the physical reasons of quenching are still largely debated and possibly related to complex baryon physics. Since the aim of TOPSEM is not to pin down the physical mechanism leading to quenching, it tries to be as agnostic as possible in regards to this problem. Therefore the monotonic relation between sSFR and sHAR is assumed to be valid only up to the moment of quenching; thereafter, stellar mass does not grow any longer, independently of the accretion history of the DM halo. Despite this, TOPSEM do keep track of passive galaxies in a fully empirical way, by following the evolution of the quiescent galaxy stellar mass function across various redshifts. In essence, the quiescent galaxy distribution describes the number of quiescent galaxies with a given stellar mass at different redshifts, and its temporal evolution provides information on the number of galaxies quenching at a specific redshift. By reproducing this distribution, TOPSEM is able to infer the number of quiescent galaxies across cosmic time and their redshift of quenching z_Q (for details see Boco et al. 2023).

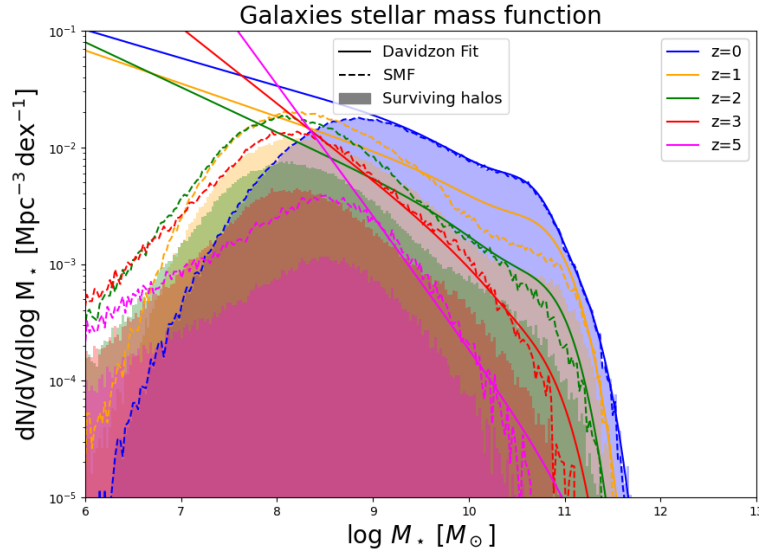


Fig. 6 Figure from Boco et al. (2023) showing the total stellar mass function evolution with redshift: blue $z = 0$, orange $z = 1$, green $z = 2$, red $z = 3$ and magenta $z = 5$. Histograms represent the stellar mass function for surviving halos, dashed lines are the total mass function reconstructed from the halo catalog and solid lines show the fit by Davidzon et al. (2017) that should be considered valid for $M_* \gtrsim$ a few $10^9 M_\odot$. In this stellar mass range, TOPSEM is able to well reproduce the evolution of stellar mass function up to $z \sim 5$.

In TOPSEM the sSFR vs. sHAR relation is derived via abundance matching without any a-priori parametrization, according to:

$$\int_{\log \text{sSFR}}^{\infty} d \log \text{sSFR}' \frac{dp}{d \log \text{sSFR}'} = \int_{-\infty}^{\infty} d \log \text{sHAR}' \frac{dp}{d \log \text{sHAR}'} \times \frac{1}{2} \operatorname{erfc} \left[\frac{\log(\text{sHAR}(\text{sSFR}, z)/\text{sHAR}')}{\sqrt{2} \sigma_{\log \text{sSFR}}} \right], \quad (1)$$

where $dp/d \log \text{sHAR}$ and $dp/d \log \text{sSFR}$ are the distributions in sHAR and sSFR. The $\text{sSFR}(\text{sHAR}, z)$ relation is derived by numerically solving Equation (1). This corresponds to finding the most suitable sSFR value for each sHAR, in order to equate the two integrals, thus matching the cumulative distributions of sSFR and sHAR. This is the essence of the abundance matching procedure. The quantity $\sigma_{\log \text{sSFR}}$ appearing at the denominator in the right-hand term represents the scatter on the relation.

Despite its simplicity, TOPSEM is able to reproduce reasonably well the evolution of the stellar population in galaxies, as shown in Figure 6 which displays the comparison between the stellar mass function for surviving halos in our catalog (histograms), the predicted stellar mass function for all the galaxies (dashed lines), and the Davidzon et al. (2017) fit to observations (solid lines; this should be considered valid for $M_* \gtrsim$ a few $10^9 M_\odot$) at different redshifts z (color code). Since at $z \approx 0$ our initial condition assigns stellar masses on the basis of the SMHM, the local stellar mass function is reproduced by construction. However, TOPSEM is able to fairly trace its evolution at all redshifts up to $z \sim 5$, where it starts lacking statistics at high stellar masses. The good match with the observed global stellar mass function at all redshifts further supports the assumption of monotonicity between sSFR and sHAR.

3.3 Testing hypothesis on morphology

In the previous Sections we have described how TOPSEM constructs a galaxy catalog by connecting halo and galaxy properties: this is the *descriptive* component of the model. Here we show how this handy model can be exploited to test a specific hypothesis for the morphological evolution of galaxies: this is the *interpretative* component of the model. The idea is extremely simple: the galactic bulge and spheroids are formed during the fast phase of DM halo growth, while disks are originated in the subsequent slow accretion phase. On this basis, the amount of stellar mass in the bulge $M_{*,b}$ and in the disk $M_{*,d}$ can be predicted for every galaxy in the catalog and directly depends on the galaxy star formation history and on the transition redshift between fast and slow accretion z_{FS} of the halo. There are three possible occurrences, which depend on the relative position of the transition redshift z_{FS} and the quenching redshift z_Q :

- $z_{\text{FS}} < 0$. There are some cases in which halos, especially massive ones, are still in the fast accretion regime at $z = 0$. In these cases all the stellar mass formed is in the bulge, i.e., the galaxy is an elliptical.
- $z_{\text{FS}} > 0$ and $z_Q > z_{\text{FS}}$. In this case the transition between fast and slow accretion occurs before $z = 0$, but the galaxy has already quenched before the transition. Also in this case all the stellar mass formed is in the bulge and the galaxy is an elliptical.
- $z_{\text{FS}} > 0$ and $z_Q < z_{\text{FS}}$. In this case the transition between fast and slow accretion occurs before $z = 0$ and quenching happens after the transition or does not happen at all. In this case all the stellar mass formed before the transition is in the bulge and the rest in the disk. The relative abundance of bulge and disk components are determined by the precise values of z_Q and z_{FS} : an early transition and no quenching would result in a galaxy with a prominent disk; a late transition, close to the quenching time, would result in a bulge-

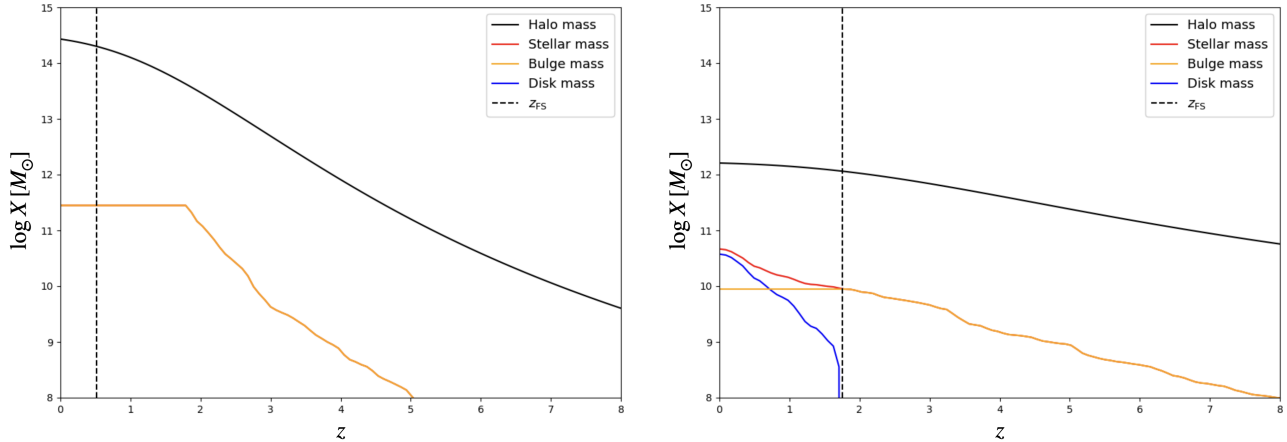


Fig. 7 Figure from Boco et al. (2023) showing examples of evolution for bulges and disks for two galaxies in TOPSEM. Black line: halo mass, red line: total stellar mass, orange line: bulge mass, blue line: disk mass. Dashed vertical line represents the transition epoch between fast and slow accretion z_{FS} . Left panel shows a quenched galaxy with $z_Q > z_{FS}$, all the stellar mass in the bulge and the galaxy is an elliptical. Right panel shows a star-forming galaxy building its bulge up to $z_{FS} \approx 1.5$ and its disk at lower redshift.

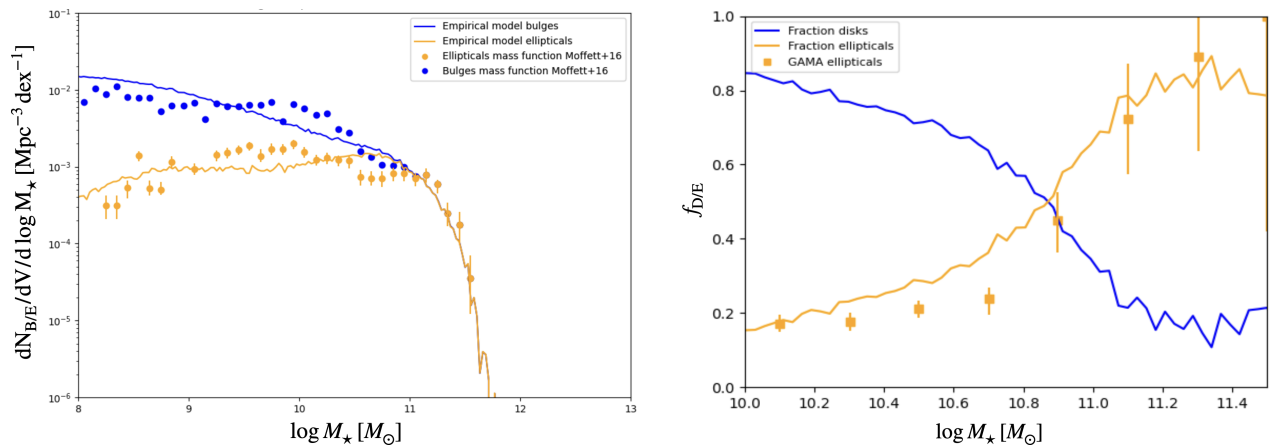


Fig. 8 Figure from Boco et al. (2023) showing the outcomes of TOPSEM. Left panel: bulge stellar mass function. Solid lines are model predictions, dots are GAMA data by Moffett et al. (2016a,b). In blue the total bulge stellar mass function, in orange the stellar mass function for ellipticals. Right panel: fraction of disks and ellipticals as a function of stellar mass at $z = 0$. Solid lines are the model results, square dots display GAMA data by Moffett et al. (2016a,b). Orange line refers to the ellipticals fraction, while the blue line to the disk fraction.

dominated/lenticular galaxy.

Two examples of the SFH of galaxies as a function of redshift can be seen in Figure 7. The bulge mass growth is shown in orange, the disk mass in blue and the total stellar mass in red. The left panel shows a case in which the fast-slow transition occurs after quenching; therefore all the stellar mass is in the bulge. In the right panel it is shown the case of a galaxy with no quenching, so that the separation between the bulge and disk components is evident. In this respect, TOPSEM can also shed light on the relation between morphology and star formation (see Section 1). As a matter of fact, elliptical galaxies are found to be more massive and quiescent, while disk galaxies are generally less massive and star-forming in the local Universe. In TOPSEM, quenching is not directly related to morphology, but a link between them naturally emerges. Indeed, the transition redshift z_{FS} , on average, decreases for higher descendant halo masses. Consequently, massive halos, typically hosting massive quiescent galaxies, have less or no time to develop a substantial stellar disk and they tend to host pure ellipticals. Contrariwise, star-forming galaxies are usually hosted in lower mass halos, which have a higher transition redshift and more time to develop a stellar disk.

It is important now to statistically evaluate the hypothesis for disk and bulge formation comparing it with the available data for galaxy morphology. In the left panel of Figure 8 it is shown the $z \approx 0$ stellar mass function for bulges and ellipticals, compared with the observational GAMA data from Moffett et al. (2016a,b): the agreement is impressive. The right panel, instead, shows the fraction of elliptical galaxies as a function of the stellar mass at $z \approx 0$ (orange line). This fraction increases with M_* , ranging from ~ 0.15 at $M_* \sim 10^{10} M_\odot$ to

~ 0.75 at $M_* \sim 10^{11} M_\odot$. Even in this case the agreement with observations is very good, at least up to $M_* \gtrsim 10^{11} M_\odot$. At higher stellar masses the fraction of ellipticals remains high but the trend in the model outputs becomes unclear. This is due at least to two reasons: (i) lack of statistics, i.e., at high stellar masses the number of galaxies per mass bin becomes very low (of the order of unity) creating a large scatter on the results; (ii) dry mergers may become important and contribute in shaping the morphology of galaxies. All in all, these results indicate that the hypothesis linking the bulge/disk dichotomy to different halo accretion modes is very promising.

4 What next?

In this Section we highlight a few aspects that have only started being considered in semi-empirical approaches and could represent future avenues of exploration or of application for next-generation SEMs.

- *Coevolution of galaxies and supermassive black holes*

The role in galaxy evolution of (super)massive black holes (BHs) with masses $M_\bullet \sim 10^{6-10} M_\odot$ constitute a crucial yet long-standing problem in modern astrophysics and cosmology. These monsters are thought to have grown mainly by gaseous accretion onto a disk surrounding the BH (e.g., Lynden-Bell 1969; Shakura and Sunyaev 1973) that energizes the spectacular broadband emission of active galactic nuclei (AGNs) and leaves a BH relic ubiquitously found at the center of massive galaxies in the local universe (e.g., Kormendy and Ho 2013). This paradigm has received a smoking gun confirmation by the Event Horizon Telescope Collaboration et al. (2019, 2022) via the imaging of the BH shadow caused by gravitational light bending and photon capture at the event horizon of M87 and Sgr A*. Observed tight relationships between the relic BH masses and the physical properties of the hosts, most noticeably the stellar mass or velocity dispersion of the bulge component (e.g., Magorrian et al. 1998; Ferrarese and Merritt 2000; Gebhardt et al. 2000; Tremaine et al. 2002; Kormendy and Ho 2013; McConnell and Ma 2013; Reines and Volonteri 2015; Shankar et al. 2016; Sahu et al. 2019; Zhu et al. 2021) suggest that the BH and the bulge stellar mass must have co-evolved over comparable timescales (see review by Alexander and Hickox 2012), possibly determined by the energy feedback from the BH itself on the gas/dust content of the host during accretion episodes (see Tinsley 1980; Silk and Rees 1998; Fabian 1999; King 2005; Shankar et al. 2006; Lapi et al. 2006, 2014, 2018; for a review, see King and Pounds 2015). Moreover, the discovery of an increasing number of active BHs with masses $M_\bullet \gtrsim 10^9 M_\odot$ at high redshifts $z \gtrsim 7$ (e.g., Mortlock et al. 2011; Wang et al. 2015, 2018; Bañados et al. 2018; Reed et al. 2019; Matsuoka et al. 2019; Yang et al. 2021a,b; for a recent review see Fan et al. 2023), when the age of the universe was shorter than 0.8 Gyr, has rekindled the attention on mechanisms able to rapidly produce heavy BH seeds of $10^{3-5} M_\odot$, thus reducing the time required to attain the final masses by standard disk accretion (see Natarajan 2014; Madau et al. 2014; Mayer and Bonoli 2019; Inayoshi et al. 2020; Boco et al. 2020, 2021b; Volonteri et al. 2021; Pacucci and Loeb 2024).

In terms of SEMs, early on the issue was addressed via a pioneering model put forward by Hopkins et al. (2006), that exploits specific AGN light curves folded with data-driven prescriptions for galaxy statistics to test hypotheses on quasar lifetimes and Eddington ratio distributions (see also Hopkins and Hernquist 2009). In recent years, the focus of SEMs on the galaxy-BH coevolution issue has been rekindled with a development of the UNIVERSEMACHINE model called TRINITY (see Zhang et al. 2023, 2024a). This descriptive SEM attempts to self-consistently infer the statistical connection between DM halos, galaxies, and supermassive BHs across cosmic times by constraining an admittedly large number of parameters (of order 60) with several galaxy and BH observables. TRINITY provides predictions for the buildup of BHs from early epochs to the present time, for the redshift-dependent relationships between BH and galaxy observables, for the clustering properties of galaxies and AGNs, etc. However, the issue about the formation of supermassive BHs and their evolution with the host galaxies is far from being solved, both from an observational and from a modeling perspective. On the observational side, it is worth mentioning two recent JWST discoveries. The first concerns the identification of some BHs that are overmassive with respect to the host galaxies at very high redshift $z \gtrsim 10$ (e.g., Goulding et al. 2023; Bogdán et al. 2024; Maiolino et al. 2024b). The second involves an overmassive, X-ray underluminous BH population at intermediate $z \sim 4-8$ (e.g., Übler et al. 2023; Furtak et al. 2023; Harikane et al. 2023; Kokorev et al. 2023; Stone et al. 2024), mostly located in the so called ‘little red dots’ sources (see Kocevski et al. 2023; Matthee et al. 2024), that could represent (lightly) dust-reddened AGNs (see Greene et al. 2024; Yue et al. 2024; Maiolino et al. 2024a); note that their number densities tends to overproduce the X-ray luminosity function at the same redshifts by up to an order of magnitude. On the modeling side, it would be extremely valuable to explore these new exciting, but also puzzling, data through the lens of interpretative and hybrid SEMs. These can verify for possible internal self-consistency among distinct datasets, whilst testing some underlying physical scenarios via flexible and transparent approaches characterized by a small numbers of parameters. Hopefully, such approaches could lead to understand better how to form overmassive BHs in the early Universe and to clarify the role of BHs in galaxy evolution.

- *Galaxy quenching mechanisms*

One of the most important and mysterious issues in galaxy evolution concerns how galaxies quench their star formation. Proposed mechanisms include: morphological quenching, possibly related to the presence of the stellar bulge (e.g., Cook et al. 2009; Martig et al. 2009; Gensior et al. 2020); negative energy/momentum feedback via stellar winds, supernova explosions and accreting supermassive BHs that can heat and eject gas from starforming regions (e.g., Silk and Rees 1998; Fabian 1999; Granato et al. 2004; King 2005; Lapi

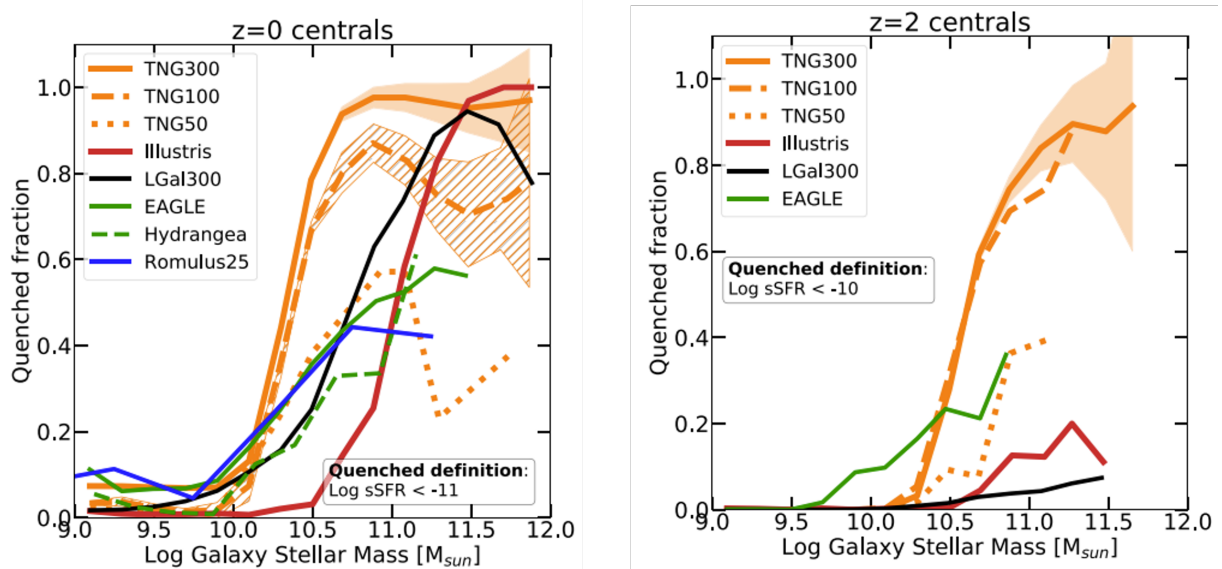


Fig. 9 Figure from Donnari et al. (2021) showing the outcomes from different theoretical models of galaxy evolution for the fraction of quiescent galaxies as a function of stellar mass at $z = 0$ (left panel) and $z = 2$ (right panel).

et al. 2006; Grand et al. 2017; Lapi et al. 2018; Valentini et al. 2020; Goubert et al. 2024); mass quenching via a threshold in halo mass above which galaxies can retain a hot gas atmosphere that hinder further cold gas inflows (e.g., Birnboim and Dekel 2003; Kereš et al. 2005; Dekel and Birnboim 2006; Dekel et al. 2009, 2023); environmental quenching via tidal and ram-pressure stripping of the gas during interactions among galaxies or between a galaxy and the diffuse environment (e.g., Larson et al. 1980; Moore et al. 1999; Bekki et al. 2002; Roediger et al. 2014; Steinhauser et al. 2016; Man and Belli 2018; Mao et al. 2022). Reasonably, all these effects could combine to various degree in galaxies with different states and environments. As of now, there is no definitive observational evidence pinpointing the leading mechanism responsible for quenching galaxies of different morphological types. Even from a theoretical perspective, ab initio approaches (like SAMs and SIMs) struggle somewhat in highlighting the primary physical mechanism responsible for quenching galaxies, and their outputs are often controversial, degenerate and strongly dependent on detailed physical recipes (e.g., Scannapieco et al. 2012; Donnari et al. 2021; Habouzit et al. 2022; Crain and van de Voort 2023). As an example, Figure 9 shows the predictions of different theoretical models of galaxy evolution for the fraction of quiescent galaxies at different stellar masses and redshifts $z \approx 0$ (left panel) and $z \approx 2$ (right panel). It appears evident that accurately reproducing the observed number density and properties of quiescent galaxies at different cosmic epochs remains an unsolved problem.

In this complex landscape, SEMs of galaxy evolution could play a pivotal role in setting more stringent constraints on the origin of quenching. The most effective route could be to design a hybrid SEM where specific quenching hypotheses are applied on top of a very basic data-driven framework, gauged on the observed statistical properties of galaxies in different states (for a first attempt see, e.g., Fu et al. 2025). Then each of the putative triggers for quenching can be systematically tested, in isolation or in combination with others, against the observed abundances and properties of quenched galaxies at different cosmic epochs. In this way the modeling would avoid becoming dependent on too many parameters and being exposed to the danger of serious degeneracies or divergences. The impact of any physical hypothesis for quenching could thus be disentangled clearly in the outcomes. Thanks to their flexibility and transparency, SEMs could also point/reveal new routes to test the input assumptions on quenching.

- *Synergy with data science techniques*

The advent of data science has revolutionized the field of galaxy evolution, making it possible to handle, store, mine and analyze the vast amounts of outputs associated to present and upcoming observational facilities and numerical studies. The related datasets are intrinsically rich in volume, variety, and often include information that cannot be easily described via traditional Bayesian likelihoods approaches. To face these challenges, astrophysicists have started relying on data-driven, machine learning, and AI-enhanced solutions; many of these could interface very well with the SEM spirit. For example, ensemble sampling algorithms like affine Markov Chain Monte Carlo (e.g., Goodman and Weare 2010; Foreman-Mackey et al. 2013), Hamiltonian Monte Carlo (e.g., Neal 2011; Betancourt and Girolami 2013), Dynamic Nested sampling (e.g., Skilling 2004; Higson et al. 2019) allow to efficiently explore the parameter space of a SEM, to optimize the agreement between the parametric model with the target datasets, and to provide a robust assessment of parameter uncertainties and degeneracies. On a more advanced perspective, AI-enhanced algorithms like deep learning (e.g., Huertas-Company and Lanusse 2023), generative adversarial networks (e.g., Goodfellow et al. 2014), variational autoencoders (e.g., Kingma and Welling 2013), normalizing flows (e.g., Dinh et al. 2014), etc. based on SEM outputs could be devised to connect galaxies and DM

halo properties, and then exploited to quickly populate large-volume SIMs (see Kamdar et al. 2016a,b; Agarwal et al. 2018; Hassan et al. 2022; Appleby et al. 2023), or even to emulate sub-grid physics in SIMs via generation of super-resolution tracer particles (e.g., Li et al. 2021; Zhang et al. 2024b).

5 Summary

Modeling galaxy formation and evolution is admittedly a very difficult task since galaxies constitute extremely complex systems, involving many processes over a huge range of time, space and energy scales. Although the precision of the astrophysical measurements are in no way comparable to other fields of ‘experimental’ physics, the amount of data is extraordinarily rich and the ensuing constraints on theoretical models are overwhelming. Solving open issues of galaxy formation and evolution therefore requires complementarity among different modeling approaches: (semi-)analytic, semi-empirical, and numerical models must be jointly exploited to refine sub-resolution physics, to choose the best parameterizations of the different processes under study, and to understand the inconsistencies and biases among observables.

In this review, we have provided a census of semi-empirical models (SEMs) of galaxy formation and evolution, stressing their value in being data-driven, easily expandable, and computationally low-cost approaches. We have highlighted different flavors of SEM, i.e. interpretative, descriptive and hybrid, discussing the peculiarities, virtues and shortcomings in each of these variants. We have also dissected a recent hybrid SEM, to describe in handy terms the techniques employed by these data-driven approaches to test simple hypotheses by marginalizing over unknown processes and avoiding heavy parameterizations. Finally, we have provided an outlook on possible future developments and applications of SEMs, related to the role of supermassive black holes in galaxy evolution, to galaxy quenching mechanisms, and to the synergy with advanced data science techniques.

Acknowledgments

We warmly thank L. Danese, H. Fu and the GOTHa team for useful discussions and helpful suggestions. This work is partially funded from the projects: “Data Science methods for MultiMessenger Astrophysics & Multi-Survey Cosmology” from the Italian Ministry of University and Research, Programmazione triennale 2021/2023 (DM n.2503 dd. 9 December 2019), Programma Congiunto Scuole; EU H2020-MSCA-ITN-2019 n. 860744 *BiD4BEST: Big Data applications for Black hole Evolution Studies* (coordinator F. Shankar); Italian Research Center on High Performance Computing Big Data and Quantum Computing (ICSC), project funded by European Union - NextGenerationEU - and National Recovery and Resilience Plan (NRRP) - Mission 4 Component 2 within the activities of Spoke 3 (Astrophysics and Cosmos Observations); European Union - NextGeneration EU, in the framework of the PRIN MUR 2022 project n. 20224JR28W “Charting unexplored avenues in Dark Matter”; INAF Large Grant 2022 funding scheme with the project “MeerKAT and LOFAR Team up: a Unique Radio Window on Galaxy/AGN co-Evolution; INAF GO-GTO Normal 2023 funding scheme with the project “Serendipitous H-ATLAS-fields Observations of Radio Extragalactic Sources (SHORES)”.

See Also: article title article title

References

- Abadi MG, Navarro JF, Steinmetz M and Eke VR (2003), Nov. Simulations of Galaxy Formation in a Λ Cold Dark Matter Universe. II. The Fine Structure of Simulated Galactic Disks. *ApJ* 597 (1): 21–34. doi:10.1086/378316. astro-ph/0212282.
- Agarwal S, Davé R and Basset BA (2018), Aug. Painting galaxies into dark matter haloes using machine learning. *MNRAS* 478 (3): 3410–3422. doi:10.1093/mnras/sty1169. 1712.03255.
- Alexander DM and Hickox RC (2012), Jun. What drives the growth of black holes? *New Atron. Rev.* 56 (4): 93–121. doi:10.1016/j.newar.2011.11.003. 1112.1949.
- Andrews BH, Weinberg DH, Schönrich R and Johnson JA (2017), Feb. Inflow, Outflow, Yields, and Stellar Population Mixing in Chemical Evolution Models. *ApJ* 835 (2), 224. doi:10.3847/1538-4357/835/2/224. 1604.08613.
- Angulo RE and Hahn O (2022), Dec. Large-scale dark matter simulations. *Living Reviews in Computational Astrophysics* 8 (1), 1. doi:10.1007/s41115-021-00013-z. 2112.05165.
- Appleby S, Davé R, Sorini D, Lovell CC and Lo K (2023), Oct. Mapping circumgalactic medium observations to theory using machine learning. *MNRAS* 525 (1): 1167–1181. doi:10.1093/mnras/stad2266. 2301.02001.
- Ascasibar Y and Gottlöber S (2008), Jun. The dynamical structure of dark matter haloes. *MNRAS* 386 (4): 2022–2030. doi:10.1111/j.1365-2966.2008.13160.x. 0802.4348.
- Aumer M, White SDM, Naab T and Scannapieco C (2013), Oct. Towards a more realistic population of bright spiral galaxies in cosmological simulations. *MNRAS* 434 (4): 3142–3164. doi:10.1093/mnras/stt1230. 1304.1559.
- Aversa R, Lapi A, de Zotti G, Shankar F and Danese L (2015), Sep. Black Hole and Galaxy Coevolution from Continuity Equation and Abundance Matching. *ApJ* 810 (1), 74. doi:10.1088/0004-637X/810/1/74. 1507.07318.
- Bañados E, Venemans BP, Mazzucchelli C, Farina EP, Walter F, Wang F, Decarli R, Stern D, Fan X, Davies FB, Hennawi JF, Simcoe RA, Turner ML, Rix HW, Yang J, Kelson DD, Rudie GC and Winters JM (2018), Jan. An 800-million-solar-mass black hole in a significantly neutral

- Universe at a redshift of 7.5. *Nature* 553 (7689): 473–476. doi:10.1038/nature25180. 1712.01860.
- Barrera M, Springel V, White SDM, Hernández-Aguayo C, Hernquist L, Frenk C, Pakmor R, Ferlito F, Hadzhiyska B, Delgado AM, Kannan R and Bose S (2023), Nov. The MillenniumTNG Project: semi-analytic galaxy formation models on the past lightcone. *MNRAS* 525 (4): 6312–6335. doi:10.1093/mnras/stad2688. 2210.10419.
- Bassini L, Rasia E, Borgani S, Granato GL, Ragone-Figueroa C, Biffi V, Ragagnin A, Dolag K, Lin W, Murante G, Napolitano NR, Taffoni G, Tornatore L and Wang Y (2020), Oct. The DIANOGA simulations of galaxy clusters: characterising star formation in protoclusters. *A&A* 642, A37. doi:10.1051/0004-6361/202038396. 2006.13951.
- Baugh CM, Lacey CG, Frenk CS, Granato GL, Silva L, Bressan A, Benson AJ and Cole S (2005), Jan. Can the faint submillimetre galaxies be explained in the Λ cold dark matter model? *MNRAS* 356 (3): 1191–1200. doi:10.1111/j.1365-2966.2004.08553.x. astro-ph/0406069.
- Baugh CM, Gonzalez-Perez V, Lagos CDP, Lacey CG, Helly JC, Jenkins A, Frenk CS, Benson AJ, Bower RG and Cole S (2019), Mar. Galaxy formation in the Planck Millennium: the atomic hydrogen content of dark matter haloes. *MNRAS* 483 (4): 4922–4937. doi:10.1093/mnras/sty3427. 1808.08276.
- Behroozi PS, Conroy C and Wechsler RH (2010), Jul. A Comprehensive Analysis of Uncertainties Affecting the Stellar Mass-Halo Mass Relation for $0 < z < 4$. *ApJ* 717 (1): 379–403. doi:10.1088/0004-637X/717/1/379. 1001.0015.
- Behroozi PS, Marchesini D, Wechsler RH, Muzzin A, Papovich C and Stefanon M (2013), Nov. Using Cumulative Number Densities to Compare Galaxies across Cosmic Time. *ApJ* 777 (1), L10. doi:10.1088/2041-8205/777/1/L10. 1308.3232.
- Behroozi P, Wechsler RH, Hearin AP and Conroy C (2019), Sep. UNIVERSEMACHINE: The correlation between galaxy growth and dark matter halo assembly from $z = 0$ –10. *MNRAS* 488 (3): 3143–3194. doi:10.1093/mnras/stz1182. 1806.07893.
- Behroozi P, Conroy C, Wechsler RH, Hearin A, Williams CC, Moster BP, Yung LYA, Somerville RS, Gottlöber S, Yepes G and Endsley R (2020), Dec. The Universe at $z < 10$: predictions for JWST from the UNIVERSEMACHINE DR1. *MNRAS* 499 (4): 5702–5718. doi:10.1093/mnras/staa3164. 2007.04988.
- Bekki K, Couch WJ and Shioya Y (2002), Oct. Passive Spiral Formation from Halo Gas Starvation: Gradual Transformation into S0s. *ApJ* 577 (2): 651–657. doi:10.1086/342221. astro-ph/0206207.
- Bellstedt S, Robotham ASG, Driver SP, Lagos CDP, Davies LJM and Cook RHW (2024), Mar. Resolving cosmic star formation histories of present-day bulges, discs, and spheroids with PROFUSE. *MNRAS* 528 (3): 5452–5476. doi:10.1093/mnras/stae394. 2307.02788.
- Benson AJ (2012), Feb. GALACTICUS: A semi-analytic model of galaxy formation. *New Astron.* 17 (2): 175–197. doi:10.1016/j.newast.2011.07.004. 1008.1786.
- Bernardi M, Meert A, Sheth RK, Fischer JL, Huertas-Company M, Maraston C, Shankar F and Vikram V (2017), May. The high mass end of the stellar mass function: Dependence on stellar population models and agreement between fits to the light profile. *MNRAS* 467 (2): 2217–2233. doi:10.1093/mnras/stx176. 1604.01036.
- Betancourt MJ and Girolami M (2013), Dec. Hamiltonian Monte Carlo for Hierarchical Models. *arXiv e-prints*, arXiv:1312.0906doi:10.48550/arXiv.1312.0906. 1312.0906.
- Béthermin M, Daddi E, Magdis G, Sargent MT, Hezaveh Y, Elbaz D, Le Borgne D, Mullaney J, Pannella M, Buat V, Charmandaris V, Lagache G and Scott D (2012), Oct. A Unified Empirical Model for Infrared Galaxy Counts Based on the Observed Physical Evolution of Distant Galaxies. *ApJ* 757 (2), L23. doi:10.1088/2041-8205/757/2/L23. 1208.6512.
- Birnboim Y and Dekel A (2003), Oct. Virial shocks in galactic haloes? *MNRAS* 345 (1): 349–364. doi:10.1046/j.1365-8711.2003.06955.x. astro-ph/0302161.
- Bisigello L, Caputi KI, Grogan N and Koekemoer A (2018), Jan. Analysis of the SFR- M^* plane at $z < 3$: single fitting versus multi-Gaussian decomposition. *A&A* 609, A82. doi:10.1051/0004-6361/201731399. 1706.06154.
- Boco L, Lapi A and Danese L (2020), Mar. Growth of Supermassive Black Hole Seeds in ETG Star-forming Progenitors: Multiple Merging of Stellar Compact Remnants via Gaseous Dynamical Friction and Gravitational-wave Emission. *ApJ* 891 (1), 94. doi:10.3847/1538-4357/ab7446. 2002.03645.
- Boco L, Lapi A, Chruslinska M, Donevski D, Sicilia A and Danese L (2021a), Feb. Evolution of Galaxy Star Formation and Metallicity: Impact on Double Compact Object Mergers. *ApJ* 907 (2), 110. doi:10.3847/1538-4357/abd3a0. 2012.02800.
- Boco L, Lapi A, Sicilia A, Capurri G, Baccigalupi C and Danese L (2021b), Oct. Growth of massive black hole seeds by migration of stellar and primordial black holes: gravitational waves and stochastic background. *JCAP* 2021 (10), 035. doi:10.1088/1475-7516/2021/10/035. 2104.07682.
- Boco L, Lapi A, Shankar F, Fu H, Gabrielli F and Sicilia A (2023), Sep. Two Parameters Semi Empirical Model (TOPSEM): Galaxy Evolution and Bulge/Disk Dichotomy from Two-stage Halo Accretion. *ApJ* 954 (1), 97. doi:10.3847/1538-4357/ace76d. 2307.13036.
- Bogdán Á, Goulding AD, Natarajan P, Kovács OE, Tremblay GR, Chadayammuri U, Volonteri M, Kraft RP, Forman WR, Jones C, Churazov E and Zhuravleva I (2024), Jan. Evidence for heavy-seed origin of early supermassive black holes from a $z \approx 10$ X-ray quasar. *Nature Astronomy* 8: 126–133. doi:10.1038/s41550-023-02111-9. 2305.15458.
- Bouché N, Dekel A, Genzel R, Genel S, Cresci G, Förster Schreiber NM, Shapiro KL, Davies RI and Tacconi L (2010), Aug. The Impact of Cold Gas Accretion Above a Mass Floor on Galaxy Scaling Relations. *ApJ* 718 (2): 1001–1018. doi:10.1088/0004-637X/718/2/1001. 0912.1858.
- Brook CB, Governato F, Roškar R, Stinson G, Brooks AM, Wadsley J, Quinn T, Gibson BK, Snaith O, Pilkington K, House E and Pontzen A (2011), Aug. Hierarchical formation of bulgeless galaxies: why outflows have low angular momentum. *MNRAS* 415 (2): 1051–1060. doi:10.1111/j.1365-2966.2011.18545.x. 1010.1004.
- Brook CB, Stinson GS, Gibson BK, Kawata D, House EL, Miranda MS, Macciò AV, Pilkington K, Roškar R, Wadsley J and Quinn TR (2012), Oct. Thin disc, thick disc and halo in a simulated galaxy. *MNRAS* 426 (1): 690–700. doi:10.1111/j.1365-2966.2012.21738.x. 1206.0740.
- Buchan S and Shankar F (2016), Oct. Setting firmer constraints on the evolution of the most massive, central galaxies from their local abundances and ages. *MNRAS* 462 (2): 2001–2010. doi:10.1093/mnras/stw1771. 1607.05732.
- Buck T, Obreja A, Macciò AV, Minchev I, Dutton AA and Ostriker JP (2020), Jan. NIHAO-UHD: the properties of MW-like stellar discs in high-resolution cosmological simulations. *MNRAS* 491 (3): 3461–3478. doi:10.1093/mnras/stz3241. 1909.05864.
- Cattaneo A, Blaizot J, Devriendt JEG, Mamon GA, Tollet E, Dekel A, Guiderdoni B, Kucukbas M and Thob ACR (2017), Oct. The new semi-analytic code GALICS 2.0 - reproducing the galaxy stellar mass function and the Tully-Fisher relation simultaneously. *MNRAS* 471 (2): 1401–1427. doi:10.1093/mnras/stx1597. 1706.07106.
- Ceverino D, Primack J, Dekel A and Kassin SA (2017), May. Formation and settling of a disc galaxy during the last 8 billion years in a cosmological simulation. *MNRAS* 467 (3): 2664–2672. doi:10.1093/mnras/stx289. 1608.02114.
- Chiappini C, Matteucci F and Gratton R (1997), Mar. The Chemical Evolution of the Galaxy: The Two-Infall Model. *ApJ* 477 (2): 765–780. doi:10.1086/303726. astro-ph/9609199.
- Chiappini C, Matteucci F and Romano D (2001), Jun. Abundance Gradients and the Formation of the Milky Way. *ApJ* 554 (2): 1044–1058. doi:10.1086/321427. astro-ph/0102134.
- Chiosi C (1980), Mar. Chemical evolution of the galactic disk: the inflow problem. *A&A* 83: 206–216.
- Cimatti A, Fraternali F and Nipoti C (2020). Introduction to galaxy formation and evolution: from primordial gas to present-day galaxies.

- Cole S, Lacey CG, Baugh CM and Frenk CS (2000), Nov. Hierarchical galaxy formation. *MNRAS* 319 (1): 168–204. doi:10.1046/j.1365-8711.2000.03879.x. astro-ph/0007281.
- Colín P, Avila-Reese V, Roca-Fàbrega S and Valenzuela O (2016), Oct. Cosmological simulations of Milky Way-sized galaxies. *ApJ* 829 (2), 98. doi:10.3847/0004-637X/829/2/98. 1607.07917.
- Conroy C and Wechsler RH (2009), May. Connecting Galaxies, Halos, and Star Formation Rates Across Cosmic Time. *ApJ* 696 (1): 620–635. doi:10.1088/0004-637X/696/1/620. 0805.3346.
- Cook M, Lapi A and Granato GL (2009), Jul. Two-phase galaxy formation. *MNRAS* 397 (1): 534–547. doi:10.1111/j.1365-2966.2009.14962.x. 0903.2390.
- Courteau S, Cappellari M, de Jong RS, Dutton AA, Emsellem E, Hoekstra H, Koopmans LVE, Mamon GA, Maraston C, Treu T and Widrow LM (2014), Jan. Galaxy masses. *Reviews of Modern Physics* 86 (1): 47–119. doi:10.1103/RevModPhys.86.47. 1309.3276.
- Cousin M, Buat V, Boissier S, Bethermin M, Roehly Y and Génou M (2016), May. Metal enrichment in a semi-analytical model, fundamental scaling relations, and the case of Milky Way galaxies. *A&A* 589, A109. doi:10.1051/0004-6361/201527734. 1602.07908.
- Cowie LL, Songaila A, Hu EM and Cohen JG (1996), Sep. New Insight on Galaxy Formation and Evolution From Keck Spectroscopy of the Hawaii Deep Fields. *AJ* 112: 839. doi:10.1086/118058. astro-ph/9606079.
- Crain RA and van de Voort F (2023), Aug. Hydrodynamical Simulations of the Galaxy Population: Enduring Successes and Outstanding Challenges. *ARA&A* 61: 473–515. doi:10.1146/annurev-astro-041923-043618. 2309.17075.
- Crain RA, Schaye J, Bower RG, Furlong M, Schaller M, Theuns T, Dalla Vecchia C, Frenk CS, McCarthy IG, Helly JC, Jenkins A, Rosas-Guevara YM, White SDM and Trayford JW (2015), Jun. The EAGLE simulations of galaxy formation: calibration of subgrid physics and model variations. *MNRAS* 450 (2): 1937–1961. doi:10.1093/mnras/stv725. 1501.01311.
- Croton DJ, Springel V, White SDM, De Lucia G, Frenk CS, Gao L, Jenkins A, Kauffmann G, Navarro JF and Yoshida N (2006), Jan. The many lives of active galactic nuclei: cooling flows, black holes and the luminosities and colours of galaxies. *MNRAS* 365 (1): 11–28. doi:10.1111/j.1365-2966.2005.09675.x. astro-ph/0508046.
- Croton DJ, Stevens ARH, Tonini C, Garel T, Bernyk M, Bibiano A, Hodkinson L, Mutch SJ, Poole GB and Shattow GM (2016), Feb. Semi-Analytic Galaxy Evolution (SAGE): Model Calibration and Basic Results. *ApJs* 222 (2), 22. doi:10.3847/0067-0049/222/2/22. 1601.04709.
- Daddi E, Dickinson M, Morrison G, Chary R, Cimatti A, Elbaz D, Frayer D, Renzini A, Pope A, Alexander DM, Bauer FE, Giavalisco M, Huynh M, Kurk J and Mignoli M (2007), Nov. Multiwavelength Study of Massive Galaxies at $z \sim 2$. I. Star Formation and Galaxy Growth. *ApJ* 670 (1): 156–172. doi:10.1086/521818. 0705.2831.
- Davé R, Finlator K and Oppenheimer BD (2012), Mar. An analytic model for the evolution of the stellar, gas and metal content of galaxies. *MNRAS* 421 (1): 98–107. doi:10.1111/j.1365-2966.2011.20148.x. 1108.0426.
- Davé R, Anglés-Alcázar D, Narayanan D, Li Q, Rafieferantsoa MH and Appleby S (2019), Jun. SIMBA: Cosmological simulations with black hole growth and feedback. *MNRAS* 486 (2): 2827–2849. doi:10.1093/mnras/stz937. 1901.10203.
- Davidzon I, Ilbert O, Laigle C, Coupon J, McCracken HJ, Delvecchio I, Masters D, Capak P, Hsieh BC, Le Fèvre O, Tresse L, Bethermin M, Chang YY, Faisst AL, Le Floc'h E, Steinhardt C, Toft S, Aussel H, Dubois C, Hasinger G, Salvato M, Sanders DB, Scoville N and Silverman JD (2017), Sep. The COSMOS2015 galaxy stellar mass function. Thirteen billion years of stellar mass assembly in ten snapshots. *A&A* 605, A70. doi:10.1051/0004-6361/201730419. 1701.02734.
- De Lucia G, Springel V, White SDM, Croton D and Kauffmann G (2006), Feb. The formation history of elliptical galaxies. *MNRAS* 366 (2): 499–509. doi:10.1111/j.1365-2966.2005.09879.x.
- Dekel A and Birnboim Y (2006), May. Galaxy bimodality due to cold flows and shock heating. *MNRAS* 368 (1): 2–20. doi:10.1111/j.1365-2966.2006.10145.x. astro-ph/0412300.
- Dekel A, Birnboim Y, Engel G, Freundlich J, Goerdt T, Mumcuoglu M, Neistein E, Pichon C, Teyssier R and Zinger E (2009), Jan. Cold streams in early massive hot haloes as the main mode of galaxy formation. *Nature* 457 (7228): 451–454. doi:10.1038/nature07648. 0808.0553.
- Dekel A, Tziperman O, Sarkar KC, Ginzburg O, Mandelker N, Ceverino D and Primack J (2023), May. Conditions for clump survival in High- z disc galaxies. *MNRAS* 521 (3): 4299–4322. doi:10.1093/mnras/stad855. 2209.04462.
- Diemand J, Kuhlen M and Madau P (2007), Oct. Formation and Evolution of Galaxy Dark Matter Halos and Their Substructure. *ApJ* 667 (2): 859–877. doi:10.1086/520573. astro-ph/0703337.
- Diemer B, More S and Kravtsov AV (2013), Mar. The Pseudo-evolution of Halo Mass. *ApJ* 766 (1), 25. doi:10.1088/0004-637X/766/1/25. 1207.0816.
- Dimauro P, Daddi E, Shankar F, Cattaneo A, Huertas-Company M, Bernardi M, Caro F, Dupke R, Häußler B, Johnston E, Cortesi A, Mei S and Peletier R (2022), Jun. Coincidence between morphology and star formation activity through cosmic time: the impact of the bulge growth. *MNRAS* 513 (1): 256–281. doi:10.1093/mnras/stac884. 2203.15819.
- Dinh L, Krueger D and Bengio Y (2014), Oct. NICE: Non-linear Independent Components Estimation. *arXiv e-prints*, arXiv:1410.8516doi:10.48550/arXiv.1410.8516. 1410.8516.
- Dome T, Tacchella S, Fialkov A, Ceverino D, Dekel A, Ginzburg O, Lapiner S and Looser TJ (2024), Jan. Mini-quenching of $z = 4-8$ galaxies by bursty star formation. *MNRAS* 527 (2): 2139–2151. doi:10.1093/mnras/stad3239. 2305.07066.
- Donnari M, Pillepich A, Nelson D, Marinacci F, Vogelsberger M and Hernquist L (2021), Oct. Quenched fractions in the IllustrisTNG simulations: comparison with observations and other theoretical models. *MNRAS* 506 (4): 4760–4780. doi:10.1093/mnras/stab1950. 2008.00004.
- Drakos NE, Villaseñor B, Robertson BE, Hausen R, Dickinson ME, Ferguson HC, Furlanetto SR, Greene JE, Madau P, Shapley AE, Stark DP and Wechsler RH (2022), Feb. Deep Realistic Extragalactic Model (DREaM) Galaxy Catalogs: Predictions for a Roman Ultra-deep Field. *ApJ* 926 (2), 194. doi:10.3847/1538-4357/ac46fb. 2110.10703.
- Driver SP, Bellstedt S, Robotham ASG, Baldry IK, Davies LJ, Liske J, Obreschkow D, Taylor EN, Wright AH, Alpaslan M, Bamford SP, Bauer AE, Bland-Hawthorn J, Bilicki M, Bravo M, Brough S, Casura S, Cluver ME, Colless M, Conselice CJ, Croom SM, de Jong J, D'Eugenio F, De Propriis R, Dogruel B, Drinkwater MJ, Dvornik A, Farrow DJ, Frenk CS, Giblin B, Graham AW, Grootes MW, Gunawardhana MLP, Hashemizadeh A, Häußler B, Heymans C, Hildebrandt H, Holwerda BW, Hopkins AM, Jarrett TH, Heath Jones D, Kelvin LS, Koushan S, Kuijken K, Lara-López MA, Lange R, López-Sánchez ÁR, Loveday J, Mahajan S, Meyer M, Moffett AJ, Napolitano NR, Norberg P, Owers MS, Radovich M, Raouf M, Peacock JA, Philipps S, Pimblett KA, Popescu C, Said K, Sansom AE, Seibert M, Sutherland WJ, Thorne JE, Tuffs RJ, Turner R, van der Wel A, van Kampen E and Wilkins SM (2022), Jun. Galaxy And Mass Assembly (GAMA): Data Release 4 and the $z \leq 0.1$ total and $z \leq 0.08$ morphological galaxy stellar mass functions. *MNRAS* 513 (1): 439–467. doi:10.1093/mnras/stac472. 2203.08539.
- Dunlop JS, McLure RJ, Biggs AD, Geach JE, Michałowski MJ, Ivison RJ, Rujopakarn W, van Kampen E, Kirkpatrick A, Pope A, Scott D, Swinbank AM, Targett TA, Aretxaga I, Austermann JE, Best PN, Bruce VA, Chapin EL, Charlot S, Cirasuolo M, Coppin K, Ellis RS, Finkelstein SL, Hayward CC, Hughes DH, Ibar E, Jagannathan P, Khochfar S, Koprowski MP, Narayanan D, Nyland K, Papovich C, Peacock JA, Rieke GH, Robertson B, Vernstrom T, Werf PPvd, Wilson GW and Yun M (2017), Apr. A deep ALMA image of the Hubble Ultra Deep Field. *MNRAS* 466 (1): 861–883. doi:10.1093/mnras/stw3088. 1606.00227.
- Dwek E (1998), Jul. The Evolution of the Elemental Abundances in the Gas and Dust Phases of the Galaxy. *ApJ* 501: 643. doi:10.1086/305829.

astro-ph/9707024.

Edmunds MG (1990), Oct. General Constraints on the Effect of Gas Flows in the Chemical Evolution of Galaxies. *MNRAS* 246: 678.

Event Horizon Telescope Collaboration, Akiyama K, Alberdi A, Alef W, Asada K, Azulay R, Baczkó AK, Ball D, Baloković M, Barrett J, Bintley D, Blackburn L, Boland W, Bouman KL, Bower GC, Bremer M, Brinkerink CD, Brissenden R, Britzen S, Broderick AE, Brogiere D, Bronzwaer T, Byun DY, Carlstrom JE, Chael A, Chan CK, Chatterjee S, Chatterjee K, Chen MT, Chen Y, Cho I, Christian P, Conway JE, Cordes JM, Crew GB, Cui Y, Davelaar J, De Laurentis M, Deane R, Dempsey J, Desvignes G, Dexter J, Doeleman SS, Eatough RP, Falcke H, Fish VL, Fomalont E, Fraga-Encinas R, Freeman WT, Friberg P, Fromm CM, Gómez JL, Galison P, Gammie CF, García R, Gentaz O, Georgiev B, Goddi C, Gold R, Gu M, Gurwell M, Hada K, Hecht MH, Hesper R, Ho LC, Ho P, Honma M, Huang CWL, Huang L, Hughes DH, Ikeda S, Inoue M, Issaoun S, James DJ, Jannuzi BT, Janssen M, Jeter B, Jiang W, Johnson MD, Jorstad S, Jung T, Karami M, Karuppusamy R, Kawashima T, Keating GK, Kettenis M, Kim JY, Kim J, Kim J, Kino M, Koay JY, Koch PM, Koyama S, Kramer M, Kramer C, Krichbaum TP, Kuo CY, Lauer TR, Lee SS, Li YR, Li Z, Lindqvist M, Liu K, Liuzzo E, Lo WP, Lobanov AP, Loinard L, Lonsdale C, Lu RS, MacDonald NR, Mao J, Markoff S, Marrone DP, Marscher AP, Martí-Vidal I, Matsushita S, Matthews LD, Medeiros L, Menten KM, Mizuno Y, Mizuno I, Moran JM, Moriyama K, Moscibrodzka M, Müller C, Nagai H, Nagar NM, Nakamura M, Narayan R, Narayanan G, Natarajan I, Neri R, Ni C, Noutsos A, Okino H, Olivares H, Ortiz-León GN, Oyama T, Özel F, Palumbo DCM, Patel N, Pen UL, Pesce DW, Piétu V, Plambeck R, PopStefanija A, Porth O, Prather B, Preciado-López JA, Psaltis D, Pu HY, Ramakrishnan V, Rao R, Rawlings MG, Raymond AW, Rezzolla L, Ripperda B, Roelofs F, Rogers A, Ros E, Rose M, Roshanineshat A, Rottmann H, Roy AL, Ruszczyk C, Ryan BR, Rygl KJL, Sánchez S, Sánchez-Argüelles D, Sasada M, Savolainen T, Schloerb FP, Schuster KF, Shao L, Shen Z, Small D, Sohn BW, Soohoo J, Tazaki F, Tiede P, Tilanus RPJ, Titus M, Toma K, Torne P, Trent T, Trippe S, Tsuda S, van Bemmell I, van Langevelde HJ, van Rossum DR, Wagner J, Wardle J, Weintraub J, Wex N, Wharton R, Wielgus M, Wong GN, Wu Q, Young K, Young A, Younsi Z, Yuan F, Yuan YF, Zensus JA, Zhao G, Zhao SS, Zhu Z, Algaba JC, Allardi A, Amestica R, Anczarski J, Bach U, Baganoff FK, Beaudoin C, Benson BA, Berthold R, Blanchard JM, Blundell R, Bustamante S, Cappallo R, Castillo-Domínguez E, Chang CC, Chang NH, Chang SC, Chen CC, Chilson R, Chuter TC, Córdoba Rosado R, Coulson IM, Crawford TM, Crowley J, David J, Derome M, Dexter M, Dornbusch S, Dudevoir KA, Dzib SA, Eckart A, Eckert C, Erickson NR, Everett WB, Faber A, Farah JR, Fath V, Folkers TW, Forbes DC, Freund R, Gómez-Ruiz AI, Gale DM, Gao F, Geertsema G, Graham DA, Greer CH, Grosslein R, Gueth F, Haggard D, Halverson NW, Han CC, Han KC, Hao J, Hasegawa Y, Henning JW, Hernández-Gómez A, Herrero-Illana R, Heyminck S, Hirota A, Hoge J, Huang YD, Impellizzeri CMV, Jiang H, Kamble A, Keisler R, Kimura K, Kono Y, Kubo D, Kuroda J, Lacasse R, Laing RA, Leitch EM, Li CT, Lin LCC, Liu CT, Liu KY, Lu LM, Marson RG, Martin-Cocher PL, Massingill KD, Matulonis C, McCoil MP, McWhirter SR, Messias H, Meyer-Zhao Z, Michalik D, Montaña A, Montgomerie W, Mora-Klein M, Muders D, Nadolski A, Navarro S, Neilsen J, Nguyen CH, Nishioka H, Norton T, Nowak MA, Nystrom G, Ogawa H, Oshiro P, Oyama T, Parsons H, Paine SN, Peñalver J, Phillips NM, Poirier M, Pradel N, Primiani RA, Raffin PA, Rahlin AS, Reiland G, Risacher C, Ruiz I, Sáez-Madaín AF, Sasselera R, Schellart P, Shaw P, Silva KM, Shiokawa H, Smith DR, Snow W, Souccar K, Sousa D, Sridharan TK, Srinivasan R, Stahm W, Stark AA, Story K, Timmer ST, Vertatschitsch L, Walther C, Wei TS, Whitehorn N, Whitney AR, Woody DP, Wouterloot JGA, Wright M, Yamaguchi P, Yu CY, Zeballos M, Zhang S and Ziurys L (2019), Apr. First M87 Event Horizon Telescope Results. I. The Shadow of the Supermassive Black Hole. *ApJ* 875 (1), L1. doi:10.3847/2041-8213/ab0ec7. 1906.11238.

Event Horizon Telescope Collaboration, Akiyama K, Alberdi A, Alef W, Algaba JC, Anantua R, Asada K, Azulay R, Bach U, Baczkó AK, Ball D, Baloković M, Barrett J, Bauböck M, Benson BA, Bintley D, Blackburn L, Blundell R, Bouman KL, Bower GC, Boyce H, Bremer M, Brinkerink CD, Brissenden R, Britzen S, Broderick AE, Brogiere D, Bronzwaer T, Bustamante S, Byun DY, Carlstrom JE, Ciccobello C, Chael A, Chan CK, Chatterjee K, Chatterjee S, Chen MT, Chen Y, Cheng X, Cho I, Christian P, Conroy NS, Conway JE, Cordes JM, Crawford TM, Crew GB, Cruz-Osorio A, Cui Y, Davelaar J, De Laurentis M, Deane R, Dempsey J, Desvignes G, Dexter J, Dhruv V, Doeleman SS, Dougal S, Dzib SA, Eatough RP, Emami R, Falcke H, Farah J, Fish VL, Fomalont E, Ford HA, Fraga-Encinas R, Freeman WT, Friberg P, Fromm CM, Fuentes A, Galison P, Gammie CF, García R, Gentaz O, Georgiev B, Goddi C, Gold R, Gómez-Ruiz AI, Gómez JL, Gu M, Gurwell M, Hada K, Haggard D, Haworth K, Hecht MH, Hesper R, Heumann D, Ho LC, Ho P, Honma M, Huang CWL, Huang L, Hughes DH, Impellizzeri CMV, Inoue M, Issaoun S, James DJ, Jannuzi BT, Janssen M, Jeter B, Jiang W, Jiménez-Rosales A, Johnson MD, Jorstad S, Joshi AV, Jung T, Karami M, Karuppusamy R, Kawashima T, Keating GK, Kettenis M, Kim DJ, Kim JY, Kim J, Kim J, Kino M, Koay JY, Kocherlakota P, Kofuji Y, Koch PM, Koyama S, Kramer M, Kramer C, Krichbaum TP, Kuo CY, La Bella N, Lauer TR, Lee D, Lee SS, Leung PK, Levis A, Li Z, Lico R, Lindahl G, Lindqvist M, Lisakov M, Liu J, Liu K, Liuzzo E, Lo WP, Lobanov AP, Loinard L, Lonsdale CJ, Lu RS, Mao J, Marchili N, Markoff S, Marrone DP, Marscher AP, Martí-Vidal I, Matsushita S, Matthews LD, Medeiros L, Menten KM, Michalik D, Mizuno I, Mizuno Y, Moran JM, Moriyama K, Moscibrodzka M, Müller C, Mus A, Musoke G, Myserlis I, Nadolski A, Nagai H, Nagar NM, Nakamura M, Narayan R, Narayanan G, Natarajan I, Nathanail A, Fuentes SN, Neilsen J, Neri R, Ni C, Noutsos A, Nowak MA, Oh J, Okino H, Olivares H, Ortiz-León GN, Oyama T, Özel F, Palumbo DCM, Paschos GF, Park J, Parsons H, Patel N, Pen UL, Pesce DW, Piétu V, Plambeck R, PopStefanija A, Porth O, Pötzl FM, Prather B, Preciado-López JA, Psaltis D, Pu HY, Ramakrishnan V, Rao R, Rawlings MG, Raymond AW, Rezzolla L, Ricarte A, Ripperda B, Roelofs F, Rogers A, Ros E, Romero-Cañizales C, Roshanineshat A, Rottmann H, Roy AL, Ruiz I, Ruszczyk C, Rygl KJL, Sánchez S, Sánchez-Argüelles D, Sánchez-Portal M, Sasada M, Satapathy K, Savolainen T, Schloerb FP, Schonfeld J, Schuster KF, Shao L, Shen Z, Small D, Sohn BW, Soohoo J, Souccar K, Sun H, Tazaki F, Tetarenko AJ, Tiede P, Tilanus RPJ, Titus M, Torne P, Traianou E, Trent T, Trippe S, Turk M, van Bemmell I, van Langevelde HJ, van Rossum DR, Vos J, Wagner J, Ward-Thompson D, Wardle J, Weintraub J, Wex N, Wharton R, Wielgus M, Wiik K, Witzel G, Wondrak MF, Wong GN, Wu Q, Yamaguchi P, Yoon D, Young A, Young K, Younsi Z, Yuan F, Yuan YF, Zensus JA, Zhang S, Zhao GY, Zhao SS, Agurto C, Allardi A, Amestica R, Araneda JP, Arriagada O, Berghuis JL, Bertarini A, Berthold R, Blanchard J, Brown K, Cárdenas M, Cantzler M, Caro P, Castillo-Domínguez E, Chan TL, Chang CC, Chang DO, Chang SH, Chang SC, Chen CC, Chilson R, Chuter TC, Ciechanowicz M, Colín-Beltrán E, Coulson IM, Crowley J, Degenaar N, Dornbusch S, Durán CA, Everett WB, Faber A, Forster K, Fuchs MM, Gale DM, Geertsema G, González E, Graham D, Gueth F, Halverson NW, Han CC, Han KC, Hasegawa Y, Hernández-Rebollar JL, Herrera C, Herrero-Illana R, Heyminck S, Hirota A, Hoge J, Hostler Schimpf SR, Howie RE, Huang YD, Jiang H, Jinchi H, John D, Kimura K, Klein T, Kubo D, Kuroda J, Kwon C, Lacasse R, Laing R, Leitch EM, Li CT, Liu CT, Liu KY, Lin LCC, Lu LM, Mac-Auliffe F, Martin-Cocher P, Matulonis C, Maute JK, Messias H, Meyer-Zhao Z, Montaña A, Montenegro-Montes F, Montgomerie W, Moreno Nolasco ME, Muders D, Nishioka H, Norton TJ, Nystrom G, Ogawa H, Olivares R, Oshiro P, Pérez-Beaupuits JP, Parra R, Phillips NM, Poirier M, Pradel N, Qiu R, Raffin PA, Rahlin AS, Ramírez J, Ressler S, Reynolds M, Rodríguez-Montoya I, Saez-Madaín AF, Santana J, Shaw P, Shirkey LE, Silva KM, Snow W, Sousa D, Sridharan TK, Stahm W, Stark AA, Test J, Torstensson K, Venegas P, Walther C, Wei TS, White C, Wieching G, Wijnands R, Wouterloot JGA, Yu CY, Yu W and Zeballos M (2022), May. First Sagittarius A* Event Horizon Telescope Results. I. The Shadow of the Supermassive Black Hole in the Center of the Milky Way. *ApJ* 930 (2), L12. doi:10.3847/2041-8213/ac6674.

Fabian AC (1999), Oct. The obscured growth of massive black holes. *MNRAS* 308 (4): L39–L43. doi:10.1046/j.1365-8711.1999.03017.x. astro-ph/9908064.

Fan X, Bañados E and Simcoe RA (2023), Aug. Quasars and the Intergalactic Medium at Cosmic Dawn. *ARA&A* 61: 373–426. doi:10.1146/annurev-astro-052920-102455. 2212.06907.

Feldmann R (2015), May. The equilibrium view on dust and metals in galaxies: Galactic outflows drive low dust-to-metal ratios in dwarf galaxies. *MNRAS* 449 (3): 3274–3292. doi:10.1093/mnras/stv552. 1412.2755.

- Feldmann R, Quataert E, Faucher-Giguère CA, Hopkins PF, Çatmabacak O, Kereš D, Bassini L, Bernardini M, Bullock JS, Cenci E, Gensior J, Liang L, Moreno J and Wetzel A (2023), Jul. FIREbox: simulating galaxies at high dynamic range in a cosmological volume. *MNRAS* 522 (3): 3831–3860. doi:10.1093/mnras/stad1205. 2205.15325.
- Ferrara A, Pallottini A and Dayal P (2023), Jul. On the stunning abundance of super-early, luminous galaxies revealed by JWST. *MNRAS* 522 (3): 3986–3991. doi:10.1093/mnras/stad1095. 2208.00720.
- Ferrara A, Pallottini A and Sommovigo L (2024), Oct. Blue Monsters at $z > 10$. Where has all their dust gone? *arXiv e-prints*, arXiv:2410.19042doi:10.48550/arXiv.2410.19042. 2410.19042.
- Ferrarese L and Merritt D (2000), Aug. A Fundamental Relation between Supermassive Black Holes and Their Host Galaxies. *ApJ* 539 (1): L9–L12. doi:10.1086/312838. astro-ph/0006053.
- Fontanot F, Monaco P, Silva L and Grazian A (2007), Dec. Reproducing the assembly of massive galaxies within the hierarchical cosmogony. *MNRAS* 382 (2): 903–914. doi:10.1111/j.1365-2966.2007.12449.x. 0709.1804.
- Fontanot F, De Lucia G, Hirschmann M, Bruzual G, Charlot S and Zibetti S (2017), Feb. Variations of the stellar initial mass function in semi-analytical models: implications for the mass assembly and the chemical enrichment of galaxies in the GAEA model. *MNRAS* 464 (4): 3812–3824. doi:10.1093/mnras/stw2612. 1606.01908.
- Fontanot F, De Lucia G, Hirschmann M, Xie L, Monaco P, Menci N, Fiore F, Feruglio C, Cristiani S and Shankar F (2020), Aug. The rise of active galactic nuclei in the galaxy evolution and assembly semi-analytic model. *MNRAS* 496 (3): 3943–3960. doi:10.1093/mnras/staa1716. 2002.10576.
- Forbes JC, Krumholz MR and Speagle JS (2019), Aug. Towards a radially resolved semi-analytic model for the evolution of disc galaxies tuned with machine learning. *MNRAS* 487 (3): 3581–3606. doi:10.1093/mnras/stz1473. 1810.12919.
- Foreman-Mackey D, Hogg DW, Lang D and Goodman J (2013), Mar. emcee: The MCMC Hammer. *PASP* 125 (925): 306. doi:10.1086/670067. 1202.3665.
- Frankel N, Sanders J, Rix HW, Ting YS and Ness M (2019), Oct. The Inside-out Growth of the Galactic Disk. *ApJ* 884 (2), 99. doi:10.3847/1538-4357/ab4254. 1909.07118.
- Fu H, Shankar F, Ayroulou M, Dickson M, Koutsouridou I, Rosas-Guevara Y, Marsden C, Brocklebank K, Bernardi M, Shiamtanis N, Williams J, Zanisi L, Allevato V, Boco L, Bonoli S, Cattaneo A, Dimauro P, Jiang F, Lapi A, Menci N, Petropoulou S and Villforth C (2022), Nov. Testing the key role of the stellar mass-halo mass relation in galaxy merger rates and morphologies via DECODE, a novel Discrete statistical sEmi-empiriCal mODEI. *MNRAS* 516 (3): 3206–3233. doi:10.1093/mnras/stac2205. 2208.00014.
- Fu H, Shankar F, Ayroulou M, Koutsouridou I, Cattaneo A, Bertemes C, Bellstedt S, Martín-Navarro I, Leja J, Allevato V, Bernardi M, Boco L, Dimauro P, Gruppioni C, Lapi A, Menci N, Muñoz Rodríguez I, Puglisi A and Alonso-Tetilla AV (2024), Jun. Unveiling the (in)consistencies among the galaxy stellar mass function, star formation histories, satellite abundances and intracluster light from a semi-empirical perspective. *arXiv e-prints*, arXiv:2406.07605doi:10.48550/arXiv.2406.07605. 2406.07605.
- Fu H, Boco L, Shankar F, Lapi A, Ayroulou M, Roberts D, Peng Y, Rodríguez-Puebla A, Yuan F, Cleland C, Mei S and Menci N (2025). Shedding light on the star formation rate-halo accretion rate connection and halo quenching mechanism via DECODE, the Discrete statistical sEmi-empiriCal mODEI. *A&A* submitted.
- Furtak LJ, Zitrin A, Plat A, Fujimoto S, Wang B, Nelson EJ, Labbé I, Bezanson R, Brammer GB, van Dokkum P, Endsley R, Glazebrook K, Greene JE, Leja J, Price SH, Smit R, Stark DP, Weaver JR, Whitaker KE, Atek H, Chevallard J, Curtis-Lake E, Dayal P, Feltre A, Franx M, Fudamoto Y, Marchesini D, Mowla LA, Pan R, Suess KA, Vidal-García A and Williams CC (2023), Aug. JWST UNCOVER: Extremely Red and Compact Object at $z_{phot} \sim 7.6$ Triply Imaged by A2744. *ApJ* 952 (2), 142. doi:10.3847/1538-4357/acde9d. 2212.10531.
- Gallazzi A, Charlot S, Brinchmann J and White SDM (2006), Aug. Ages and metallicities of early-type galaxies in the Sloan Digital Sky Survey: new insight into the physical origin of the colour-magnitude and the $Mg_2-\sigma_V$ relations. *MNRAS* 370 (3): 1106–1124. doi:10.1111/j.1365-2966.2006.10548.x. astro-ph/0605300.
- Gebhardt K, Bender R, Bower G, Dressler A, Faber SM, Filippenko AV, Green R, Grillmair C, Ho LC, Kormendy J, Lauer TR, Magorrian J, Pinkney J, Richstone D and Tremaine S (2000), Aug. A Relationship between Nuclear Black Hole Mass and Galaxy Velocity Dispersion. *ApJ* 539 (1): L13–L16. doi:10.1086/312840. astro-ph/0006289.
- Gensior J, Kruijssen JMD and Keller BW (2020), Jun. Heart of darkness: the influence of galactic dynamics on quenching star formation in galaxy spheroids. *MNRAS* 495 (1): 199–223. doi:10.1093/mnras/staa1184. 2002.01484.
- Goodfellow IJ, Pouget-Abadie J, Mirza M, Xu B, Warde-Farley D, Ozair S, Courville A and Bengio Y (2014), Jun. Generative Adversarial Networks. *arXiv e-prints*, arXiv:1406.2661doi:10.48550/arXiv.1406.2661. 1406.2661.
- Goodman J and Weare J (2010), Jan. Ensemble samplers with affine invariance. *Communications in Applied Mathematics and Computational Science* 5 (1): 65–80. doi:10.2140/camcos.2010.5.65.
- Goubert PH, Bluck AFL, Piotrowska JM and Maiolino R (2024), Mar. The role of environment and AGN feedback in quenching local galaxies: comparing cosmological hydrodynamical simulations to the SDSS. *MNRAS* 528 (3): 4891–4921. doi:10.1093/mnras/stae269. 2401.12953.
- Goulding AD, Greene JE, Setton DJ, Labbe I, Bezanson R, Miller TB, Atek H, Bogdán Á, Brammer G, Chemerynska I, Cutler SE, Dayal P, Fudamoto Y, Fujimoto S, Furtak LJ, Kokorev V, Khullar G, Leja J, Marchesini D, Natarajan P, Nelson E, Oesch PA, Pan R, Papovich C, Price SH, van Dokkum P, Wang B, Weaver JR, Whitaker KE and Zitrin A (2023), Sep. UNCOVER: The Growth of the First Massive Black Holes from JWST/NIRSpec-Spectroscopic Redshift Confirmation of an X-Ray Luminous AGN at $z = 10.1$. *ApJ* 955 (1), L24. doi:10.3847/2041-8213/acf7c5. 2308.02750.
- Governato F, Brook C, Mayer L, Brooks A, Rhee G, Wadsley J, Jonsson P, Willman B, Stinson G, Quinn T and Madau P (2010), Jan. Bulgeless dwarf galaxies and dark matter cores from supernova-driven outflows. *Nature* 463 (7278): 203–206. doi:10.1038/nature08640. 0911.2237.
- Granato GL, De Zotti G, Silva L, Bressan A and Danese L (2004), Jan. A Physical Model for the Coevolution of QSOs and Their Spheroidal Hosts. *ApJ* 600 (2): 580–594. doi:10.1086/379875. astro-ph/0307202.
- Grand RJJ, Gómez FA, Marinacci F, Pakmor R, Springel V, Campbell DJR, Frenk CS, Jenkins A and White SDM (2017), May. The Auriga Project: the properties and formation mechanisms of disc galaxies across cosmic time. *MNRAS* 467 (1): 179–207. doi:10.1093/mnras/stx071. 1610.01159.
- Grand RJJ, van de Voort F, Zjupa J, Fragkoudi F, Gómez FA, Kauffmann G, Marinacci F, Pakmor R, Springel V and White SDM (2019), Dec. Gas accretion and galactic fountain flows in the Auriga cosmological simulations: angular momentum and metal redistribution. *MNRAS* 490 (4): 4786–4803. doi:10.1093/mnras/stz2928. 1909.04038.
- Greene JE, Labbe I, Goulding AD, Furtak LJ, Chemerynska I, Kokorev V, Dayal P, Volonteri M, Williams CC, Wang B, Setton DJ, Burgasser AJ, Bezanson R, Atek H, Brammer G, Cutler SE, Feldmann R, Fujimoto S, Glazebrook K, de Graaff A, Khullar G, Leja J, Marchesini D, Maseda MV, Matthee J, Miller TB, Naidu RP, Nanayakkara T, Oesch PA, Pan R, Papovich C, Price SH, van Dokkum P, Weaver JR, Whitaker KE and Zitrin A (2024), Mar. UNCOVER Spectroscopy Confirms the Surprising Ubiquity of Active Galactic Nuclei in Red Sources at $z \lesssim 5$. *ApJ* 964 (1), 39. doi:10.3847/1538-4357/ad1e5f. 2309.05714.
- Grisoni V, Spitoni E, Matteucci F, Recio-Blanco A, de Laverny P, Hayden M, Mikolaitis Š and Worley CC (2017), Dec. The AMBRE project:

- chemical evolution models for the Milky Way thick and thin discs. *MNRAS* 472 (3): 3637–3647. doi:10.1093/mnras/stx2201. 1706.02614.
- Grisoni V, Spitoni E and Matteucci F (2018), Dec. Abundance gradients along the Galactic disc from chemical evolution models. *MNRAS* 481 (2): 2570–2580. doi:10.1093/mnras/sty2444. 1805.11415.
- Grylls PJ, Shankar F, Zanisi L and Bernardi M (2019), Feb. A statistical semi-empirical model: satellite galaxies in groups and clusters. *MNRAS* 483 (2): 2506–2523. doi:10.1093/mnras/sty3281. 1812.00015.
- Grylls PJ, Shankar F, Leja J, Menci N, Moster B, Behroozi P and Zanisi L (2020), Jan. Predicting fully self-consistent satellite richness, galaxy growth, and star formation rates from the STatistical sEmi-Empirical modeL STEEL. *MNRAS* 491 (1): 634–654. doi:10.1093/mnras/stz2956. 1910.08417.
- Guedes J, Callegari S, Madau P and Mayer L (2011), Dec. Forming Realistic Late-type Spirals in a Λ CDM Universe: The Eris Simulation. *ApJ* 742 (2), 76. doi:10.1088/0004-637X/742/2/76. 1103.6030.
- Habouzit M, Onoue M, Bañados E, Neeleman M, Anglés-Alcázar D, Walter F, Pillepich A, Davé R, Jahnke K and Dubois Y (2022), Apr. Co-evolution of massive black holes and their host galaxies at high redshift: discrepancies from six cosmological simulations and the key role of JWST. *MNRAS* 511 (3): 3751–3767. doi:10.1093/mnras/stac225. 2201.09892.
- Harikane Y, Zhang Y, Nakajima K, Ouchi M, Isobe Y, Ono Y, Hatano S, Xu Y and Umeda H (2023), Dec. A JWST/NIRSpec First Census of Broad-line AGNs at $z = 4$ –7: Detection of 10 Faint AGNs with $M_{BH} 10^6$ – $10^8 M_{\odot}$ and Their Host Galaxy Properties. *ApJ* 959 (1), 39. doi:10.3847/1538-4357/ad029e. 2303.11946.
- Hartwick FDA (1976), Oct. The Chemical Evolution of the Galactic Halo. *ApJ* 209: 418–423. doi:10.1086/154735.
- Hassan S, Villaescusa-Navarro F, Wandelt B, Spergel DN, Anglés-Alcázar D, Genel S, Cranmer M, Bryan GL, Davé R, Somerville RS, Eickenberg M, Narayanan D, Ho S and Andrianomena S (2022), Oct. HIFLOW: Generating Diverse HI Maps and Inferring Cosmology while Marginalizing over Astrophysics Using Normalizing Flows. *ApJ* 937 (2), 83. doi:10.3847/1538-4357/ac8b09. 2110.02983.
- Hayward CC, Sparre M, Chapman SC, Hernquist L, Nelson D, Pakmor R, Pillepich A, Springel V, Vogelsberger M and Weinberger R (2021), Apr. Submillimetre galaxies in cosmological hydrodynamical simulations - an opportunity for constraining feedback models. *MNRAS* 502 (2): 2922–2933. doi:10.1093/mnras/stab246. 2007.01885.
- Hearin AP, Chaves-Montero J, Becker MR and Alarcon A (2021), Jul. A Differentiable Model of the Assembly of Individual and Populations of Dark Matter Halos. *The Open Journal of Astrophysics* 4 (1), 7. doi:10.21105/astro.2105.05859. 2105.05859.
- Hearin AP, Ramachandra N, Becker MR and DeRose J (2022), Feb. Differentiable Predictions for Large Scale Structure with SHAMNet. *The Open Journal of Astrophysics* 5, 3. doi:10.21105/astro.2112.08423. 2112.08423.
- Henriques BMB, White SDM, Thomas PA, Angulo R, Guo Q, Lemson G, Springel V and Overzier R (2015), Aug. Galaxy formation in the Planck cosmology - I. Matching the observed evolution of star formation rates, colours and stellar masses. *MNRAS* 451 (3): 2663–2680. doi:10.1093/mnras/stv705. 1410.0365.
- Henriques BMB, Yates RM, Fu J, Guo Q, Kauffmann G, Srisawat C, Thomas PA and White SDM (2020), Feb. L-GALAXIES 2020: Spatially resolved cold gas phases, star formation, and chemical enrichment in galactic discs. *MNRAS* 491 (4): 5795–5814. doi:10.1093/mnras/stz3233. 2003.05944.
- Higson E, Handley W, Hobson M and Lasenby A (2019), Sep. Dynamic nested sampling: an improved algorithm for parameter estimation and evidence calculation. *Statistics and Computing* 29 (5): 891–913. doi:10.1007/s11222-018-9844-0. 1704.03459.
- Hirashita H (2000), Aug. Dust Growth Timescale and Mass Function of Molecular Clouds in the Galaxy. *PASJ* 52: 585–588. doi:10.1093/pasj/52.4.585.
- Hirschmann M, De Lucia G and Fontanot F (2016), Sep. Galaxy assembly, stellar feedback and metal enrichment: the view from the GAEA model. *MNRAS* 461 (2): 1760–1785. doi:10.1093/mnras/stw1318. 1512.04531.
- Hoffman Y, Romano-Díaz E, Shlosman I and Heller C (2007), Dec. Evolution of the Phase-Space Density in Dark Matter Halos. *ApJ* 671 (2): 1108–1114. doi:10.1086/523695. 0706.0006.
- Hopkins PF and Hernquist L (2009), Jun. Quasars Are Not Light Bulbs: Testing Models of Quasar Lifetimes with the Observed Eddington Ratio Distribution. *ApJ* 698 (2): 1550–1569. doi:10.1088/0004-637X/698/2/1550. 0809.3789.
- Hopkins PF, Hernquist L, Cox TJ, Di Matteo T, Robertson B and Springel V (2006), Mar. A Unified, Merger-driven Model of the Origin of Starbursts, Quasars, the Cosmic X-Ray Background, Supermassive Black Holes, and Galaxy Spheroids. *ApJS* 163 (1): 1–49. doi:10.1086/499298. astro-ph/0506398.
- Hopkins PF, Kereš D, Oñorbe J, Faucher-Giguère CA, Quataert E, Murray N and Bullock JS (2014), Nov. Galaxies on FIRE (Feedback In Realistic Environments): stellar feedback explains cosmologically inefficient star formation. *MNRAS* 445 (1): 581–603. doi:10.1093/mnras/stu1738. 1311.2073.
- Hopkins PF, Wetzel A, Kereš D, Faucher-Giguère CA, Quataert E, Boylan-Kolchin M, Murray N, Hayward CC, Garrison-Kimmel S, Hummels C, Feldmann R, Torrey P, Ma X, Anglés-Alcázar D, Su KY, Orr M, Schmitz D, Escala I, Sanderson R, Grudić MY, Hafen Z, Kim JH, Fitts A, Bullock JS, Wheeler C, Chan TK, Elbert OD and Narayanan D (2018), Oct. FIRE-2 simulations: physics versus numerics in galaxy formation. *MNRAS* 480 (1): 800–863. doi:10.1093/mnras/sty1690. 1702.06148.
- Huang R, Battisti AJ, Grasha K, da Cunha E, Lagos CdP, Leslie SK and Wisnioski E (2023), Mar. Exploring the intrinsic scatter of the star-forming galaxy main sequence at redshift 0.5 to 3.0. *MNRAS* 520 (1): 446–460. doi:10.1093/mnras/stad108. 2301.01995.
- Huertas-Company M and Lanusse F (2023), Jan. The Dawes Review 10: The impact of deep learning for the analysis of galaxy surveys. *PASA* 40, e001. doi:10.1017/pasa.2022.55. 2210.01813.
- Ilbert O, McCracken HJ, Le Fèvre O, Capak P, Dunlop J, Karim A, Renzini MA, Caputi K, Boissier S, Arnouts S, Aussel H, Comparat J, Guo Q, Hudelot P, Kartaltepe J, Kneib JP, Krogager JK, Le Floc'h E, Lilly S, Mellier Y, Milvang-Jensen B, Moutard T, Onodera M, Richard J, Salvato M, Sanders DB, Scoville N, Silverman JD, Taniguchi Y, Tasca L, Thomas R, Toft S, Tresse L, Vergani D, Wolk M and Zirm A (2013), Aug. Mass assembly in quiescent and star-forming galaxies since $z \sim 4$ from UltraVISTA. *A&A* 556, A55. doi:10.1051/0004-6361/201321100. 1301.3157.
- Ilbert O, Arnouts S, Le Floc'h E, Aussel H, Bethermin M, Capak P, Hsieh BC, Kajisawa M, Karim A, Le Fèvre O, Lee N, Lilly S, McCracken HJ, Michel-Dansac L, Moutard T, Renzini MA, Salvato M, Sanders DB, Scoville N, Sheth K, Silverman JD, Smolčić V, Taniguchi Y and Tresse L (2015), Jul. Evolution of the specific star formation rate function at $z_j 1.4$ Dissecting the mass-SFR plane in COSMOS and GOODS. *A&A* 579, A2. doi:10.1051/0004-6361/201425176. 1410.4875.
- Inayoshi K, Visbal E and Haiman Z (2020), Aug. The Assembly of the First Massive Black Holes. *ARA&A* 58: 27–97. doi:10.1146/annurev-astro-120419-014455. 1911.05791.
- Inoue AK (2003), Oct. Evolution of Dust-to-Metal Ratio in Galaxies. *PASJ* 55: 901–909. doi:10.1093/pasj/55.5.901. astro-ph/0308204.
- Jeong TB, Jeon M, Song H and Bromm V (2024), Nov. Simulating high-redshift galaxies: Enhancing UV luminosity with star formation efficiency and a top-heavy IMF. *arXiv e-prints*, arXiv:2411.170072411. 17007.
- Johansson J, Thomas D and Maraston C (2012), Apr. Chemical element ratios of Sloan Digital Sky Survey early-type galaxies. *MNRAS* 421 (3): 1908–1926. doi:10.1111/j.1365-2966.2011.20316.x. 1112.0322.
- Kamdar HM, Turk MJ and Brunner RJ (2016a), Jan. Machine learning and cosmological simulations - I. Semi-analytical models. *MNRAS* 455

- (1): 642–658. doi:10.1093/mnras/stv2310. 1510.06402.
- Kamdar HM, Turk MJ and Brunner RJ (2016b), Apr. Machine learning and cosmological simulations - II. Hydrodynamical simulations. *MNRAS* 457 (2): 1162–1179. doi:10.1093/mnras/stv2981. 1510.07659.
- Katz N and Gunn JE (1991), Aug. Dissipational Galaxy Formation. I. Effects of Gasdynamics. *ApJ* 377: 365. doi:10.1086/170367.
- Kauffmann G, White SDM and Guiderdoni B (1993), Sep. The formation and evolution of galaxies within merging dark matter haloes. *MNRAS* 264: 201–218. doi:10.1093/mnras/264.1.201.
- Kereš D, Katz N, Weinberg DH and Davé R (2005), Oct. How do galaxies get their gas? *MNRAS* 363 (1): 2–28. doi:10.1111/j.1365-2966.2005.09451.x. astro-ph/0407095.
- King A (2005), Dec. The AGN-Starburst Connection, Galactic Superwinds, and $M_{BH-\sigma}$. *ApJL* 635 (2): L121–L123. doi:10.1086/499430. astro-ph/0511034.
- King A and Pounds K (2015), Aug. Powerful Outflows and Feedback from Active Galactic Nuclei. *ARA&A* 53: 115–154. doi:10.1146/annurev-astro-082214-122316. 1503.05206.
- Kingma DP and Welling M (2013), Dec. Auto-Encoding Variational Bayes. *arXiv e-prints*, arXiv:1312.6114doi:10.48550/arXiv.1312.6114. 1312.6114.
- Kocevski DD, Onoue M, Inayoshi K, Trump JR, Arrabal Haro P, Grazian A, Dickinson M, Finkelstein SL, Kartaltepe JS, Hirschmann M, Aird J, Holwerda BW, Fujimoto S, Juneau S, Amorín RO, Backhaus BE, Bagley MB, Barro G, Bell EF, Bisigello L, Calabrò A, Cleri NJ, Cooper MC, Ding X, Groggin NA, Ho LC, Hutchison TA, Inoue AK, Jiang L, Jones B, Koekemoer AM, Li W, Li Z, McGrath EJ, Molina J, Papovich C, Pérez-González PG, Pirzkal N, Wilkins SM, Yang G and Yung LYA (2023), Sep. Hidden Little Monsters: Spectroscopic Identification of Low-mass, Broad-line AGNs at $z \lesssim 5$ with CEERS. *ApJ* 954 (1), L4. doi:10.3847/2041-8213/ace5a0. 2302.00012.
- Kokorev V, Fujimoto S, Labbe I, Greene JE, Bezanson R, Dayal P, Nelson EJ, Atek H, Brammer G, Caputi KI, Chemerynska I, Cutler SE, Feldmann R, Fudamoto Y, Furtak LJ, Goulding AD, de Graaff A, Leja J, Marchesini D, Miller TB, Nanayakkara T, Oesch PA, Pan R, Price SH, Setton DJ, Smit R, Stefanon M, Wang B, Weaver JR, Whitaker KE, Williams CC and Zitrin A (2023), Nov. UNCOVER: A NIRSpec Identification of a Broad-line AGN at $z = 8.50$. *ApJ* 957 (1), L7. doi:10.3847/2041-8213/ad037a. 2308.11610.
- Kormendy J and Ho LC (2013), Aug. Coevolution (Or Not) of Supermassive Black Holes and Host Galaxies. *ARA&A* 51 (1): 511–653. doi:10.1146/annurev-astro-082708-101811. 1304.7762.
- Koutsouridou I and Cattaneo A (2022), Nov. Probing the link between quenching and morphological evolution. *MNRAS* 516 (3): 4194–4211. doi:10.1093/mnras/stac2240. 2209.12883.
- Lacey C and Cole S (1993), Jun. Merger rates in hierarchical models of galaxy formation. *MNRAS* 262 (3): 627–649. doi:10.1093/mnras/262.3.627.
- Lacey CG, Baugh CM, Frenk CS, Benson AJ, Bower RG, Cole S, Gonzalez-Perez V, Helly JC, Lagos CDP and Mitchell PD (2016), Nov. A unified multiwavelength model of galaxy formation. *MNRAS* 462 (4): 3854–3911. doi:10.1093/mnras/stw1888. 1509.08473.
- Lagos CDP, Tobar RJ, Robotham ASG, Obreschkow D, Mitchell PD, Power C and Elahi PJ (2018), Dec. Shark: introducing an open source, free, and flexible semi-analytic model of galaxy formation. *MNRAS* 481 (3): 3573–3603. doi:10.1093/mnras/sty2440. 1807.11180.
- Lah P, Scott N, Barone TM, Robotham ASG, D'Eugenio F, Colless M and Casura S (2023), Jan. Comparison of the stellar populations of bulges and discs using the MaNGA survey. *PASA* 40, e002. doi:10.1017/pasa.2022.58. 2212.06284.
- Lapi A, Shankar F, Mao J, Granato GL, Silva L, De Zotti G and Danese L (2006), Oct. Quasar Luminosity Functions from Joint Evolution of Black Holes and Host Galaxies. *ApJ* 650 (1): 42–56. doi:10.1086/507122. astro-ph/0603819.
- Lapi A, Raimundo S, Aversa R, Cai ZY, Negrello M, Celotti A, De Zotti G and Danese L (2014), Feb. The Coevolution of Supermassive Black Holes and Massive Galaxies at High Redshift. *ApJ* 782 (2), 69. doi:10.1088/0004-637X/782/2/69. 1312.3751.
- Lapi A, Pantoni L, Zanisi L, Shi J, Mancuso C, Massardi M, Shankar F, Bressan A and Danese L (2018), Apr. The Dramatic Size and Kinematic Evolution of Massive Early-type Galaxies. *ApJ* 857 (1), 22. doi:10.3847/1538-4357/aab6af. 1803.04734.
- Lapi A, Pantoni L, Boco L and Danese L (2020), Jul. New Analytic Solutions for Galaxy Evolution. II. Wind Recycling, Galactic Fountains, and Late-type Galaxies. *ApJ* 897 (1), 81. doi:10.3847/1538-4357/ab9812. 2006.01643.
- Lapi A, Boco L, Perrotta F and Massardi M (2024a), Aug. Semi-Empirical Estimates of the Cosmic Planet Formation Rate. *Galaxies* 12 (4), 49. doi:10.3390/galaxies12040049. 2408.08611.
- Lapi A, Gandolfi G, Boco L, Gabrielli F, Massardi M, Haridasu BS, Baccigalupi C, Bressan A and Danese L (2024b), Mar. Constraining the Initial Mass Function in the Epoch of Reionization from Astrophysical and Cosmological Data. *Universe* 10 (3), 141. doi:10.3390/universe10030141. 2403.07401.
- Larson RB, Tinsley BM and Caldwell CN (1980), May. The evolution of disk galaxies and the origin of S0 galaxies. *ApJ* 237: 692–707. doi:10.1086/157917.
- Li Y, Ni Y, Croft RAC, Di Matteo T, Bird S and Feng Y (2021), May. AI-assisted superresolution cosmological simulations. *Proceedings of the National Academy of Science* 118 (19), e2022038118. doi:10.1073/pnas.2022038118. 2010.06608.
- Libeskind NI, van de Weygaert R, Cautun M, Falck B, Tempel E, Abel T, Alpaslan M, Aragón-Calvo MA, Forero-Romero JE, Gonzalez R, Gottlöber S, Hahn O, Hellwing WA, Hoffman Y, Jones BJT, Kitaura F, Knebe A, Manti S, Neyrinck M, Nuza SE, Padilla N, Platen E, Ramachandra N, Robotham A, Saar E, Shandarin S, Steinmetz M, Stoica RS, Sousbie T and Yepes G (2018), Jan. Tracing the cosmic web. *MNRAS* 473 (1): 1195–1217. doi:10.1093/mnras/stx1976. 1705.03021.
- Lilly SJ, Carollo CM, Pipino A, Renzini A and Peng Y (2013), Aug. Gas Regulation of Galaxies: The Evolution of the Cosmic Specific Star Formation Rate, the Metallicity-Mass-Star-formation Rate Relation, and the Stellar Content of Halos. *ApJ* 772 (2), 119. doi:10.1088/0004-637X/772/2/119. 1303.5059.
- Lovell CC, Vijayan AP, Thomas PA, Wilkins SM, Barnes DJ, Irodotou D and Roper W (2021), Jan. First Light And Reionization Epoch Simulations (FLARES) - I. Environmental dependence of high-redshift galaxy evolution. *MNRAS* 500 (2): 2127–2145. doi:10.1093/mnras/staa3360. 2004.07283.
- Lustig P, Strazzullo V, Remus RS, D'Eugenio C, Daddi E, Burkert A, De Lucia G, Delvecchio I, Dolag K, Fontanot F, Gobat R, Mohr JJ, Onodera M, Pannella M and Pillepich A (2023), Feb. Massive quiescent galaxies at $z \approx 3$: A comparison of selection, stellar population, and structural properties with simulation predictions. *MNRAS* 518 (4): 5953–5975. doi:10.1093/mnras/stac3450. 2201.09068.
- Lynden-Bell D (1969), Aug. Galactic Nuclei as Collapsed Old Quasars. *Nature* 223 (5207): 690–694. doi:10.1038/223690a0.
- Madau P, Haardt F and Dotti M (2014), Apr. Super-critical Growth of Massive Black Holes from Stellar-mass Seeds. *ApJL* 784 (2), L38. doi:10.1088/2041-8205/784/2/L38. 1402.6995.
- Magorrian J, Tremaine S, Richstone D, Bender R, Bower G, Dressler A, Faber SM, Gebhardt K, Green R, Grillmair C, Kormendy J and Lauer T (1998), Jun. The Demography of Massive Dark Objects in Galaxy Centers. *AJ* 115 (6): 2285–2305. doi:10.1086/300353. astro-ph/9708072.
- Maiolino R and Mannucci F (2019), Feb. De re metallica: the cosmic chemical evolution of galaxies. *A&A* 27 (1), 3. doi:10.1007/s00159-018-0112-2. 1811.09642.
- Maiolino R, Scholtz J, Curtis-Lake E, Carniani S, Baker W, de Graaff A, Tacchella S, Übler H, D'Eugenio F, Witstok J, Curti M, Arribas S, Bunker AJ, Charlot S, Chevallard J, Eisenstein DJ, Egami E, Ji Z, Jones GC, Lyu J, Rawle T, Robertson B, Rujopakarn W, Perna M, Sun F, Venturi

- G, Williams CC and Willott C (2024a), Nov. JADES: The diverse population of infant black holes at $4 < z < 11$: Merging, tiny, poor, but mighty. *A&A* 691, A145. doi:10.1051/0004-6361/202347640. 2308.01230.
- Maiolino R, Scholtz J, Witstok J, Carniani S, D'Eugenio F, de Graaff A, Übler H, Tacchella S, Curtis-Lake E, Arribas S, Bunker A, Charlot S, Chevallard J, Curti M, Looser TJ, Maseda MV, Rawle TD, Rodríguez del Pino B, Willott CJ, Egami E, Eisenstein DJ, Hainline KN, Robertson B, Williams CC, Willmer CNA, Baker WM, Boyett K, DeCoursey C, Fabian AC, Helton JM, Ji Z, Jones GC, Kumari N, Laporte N, Nelson EJ, Perna M, Sandles L, Shvaei I and Sun F (2024b), Mar. A small and vigorous black hole in the early Universe. *Nature* 627 (8002): 59–63. doi:10.1038/s41586-024-07052-5. 2305.12492.
- Man A and Belli S (2018), Sep. Star formation quenching in massive galaxies. *Nature Astronomy* 2: 695–697. doi:10.1038/s41550-018-0558-1. 1809.00722.
- Mancuso C, Lapi A, Shi J, Cai ZY, Gonzalez-Nuevo J, Béthermin M and Danese L (2016a), Dec. The Main Sequences of Star-forming Galaxies and Active Galactic Nuclei at High Redshift. *ApJ* 833 (2), 152. doi:10.3847/1538-4357/833/2/152. 1610.05910.
- Mancuso C, Lapi A, Shi J, Gonzalez-Nuevo J, Aversa R and Danese L (2016b), Jun. The Quest for Dusty Star-forming Galaxies at High Redshift $z \geq 4$. *ApJ* 823 (2), 128. doi:10.3847/0004-637X/823/2/128. 1604.02507.
- Mancuso C, Lapi A, Prandoni I, Obi I, Gonzalez-Nuevo J, Perrotta F, Bressan A, Celotti A and Danese L (2017), Jun. Galaxy Evolution in the Radio Band: The Role of Star-forming Galaxies and Active Galactic Nuclei. *ApJ* 842 (2), 95. doi:10.3847/1538-4357/aa745d. 1705.06539.
- Mandelbaum R, Wang W, Zu Y, White S, Henriques B and More S (2016), Apr. Strong bimodality in the host halo mass of central galaxies from galaxy-galaxy lensing. *MNRAS* 457 (3): 3200–3218. doi:10.1093/mnras/stw188. 1509.06762.
- Mao Z, Kodama T, Pérez-Martínez JM, Suzuki TL, Yamamoto N and Adachi K (2022), Oct. Revealing impacts of stellar mass and environment on galaxy quenching. *A&A* 666, A141. doi:10.1051/0004-6361/202243733. 2208.00722.
- Martig M, Bournaud F, Teysseier R and Dekel A (2009), Dec. Morphological Quenching of Star Formation: Making Early-Type Galaxies Red. *ApJ* 707 (1): 250–267. doi:10.1088/0004-637X/707/1/250. 0905.4669.
- Martín-Navarro I, Vazdekis A, Falcón-Barroso J, La Barbera F, Yıldırım A and van de Ven G (2018), Apr. Timing the formation and assembly of early-type galaxies via spatially resolved stellar populations analysis. *MNRAS* 475 (3): 3700–3729. doi:10.1093/mnras/stx3346. 1801.05486.
- Martizzi D, Vogelsberger M, Artales MC, Haider M, Torrey P, Marinacci F, Nelson D, Pillepich A, Weinberger R, Hernquist L, Naiman J and Springel V (2019), Jul. Baryons in the Cosmic Web of IllustrisTNG - I: gas in knots, filaments, sheets, and voids. *MNRAS* 486 (3): 3766–3787. doi:10.1093/mnras/stz1106. 1810.01883.
- Matsuoka Y, Iwasawa K, Onoue M, Kashikawa N, Strauss MA, Lee CH, Imanishi M, Nagao T, Akiyama M, Asami N, Bosch J, Furusawa H, Goto T, Gunn JE, Harikane Y, Ikeda H, Izumi T, Kawaguchi T, Kato N, Kikuta S, Kohno K, Komiyama Y, Koyama S, Lupton RH, Minezaki T, Miyazaki S, Murayama H, Niida M, Nishizawa AJ, Noboriguchi A, Oguri M, Ono Y, Ouchi M, Price PA, Sameshima H, Schulze A, Silverman JD, Sugiyama N, Tait PJ, Takada M, Takata T, Tanaka M, Tang JJ, Toba Y, Utsumi Y, Wang SY and Yamashita T (2019), Oct. Subaru High- z Exploration of Low-luminosity Quasars (SHELLQs). X. Discovery of 35 Quasars and Luminous Galaxies at $5.7 \leq z \leq 7.0$. *ApJ* 883 (2), 183. doi:10.3847/1538-4357/ab3c60. 1908.07910.
- Matteucci F (2012). Chemical Evolution of Galaxies. doi:10.1007/978-3-642-22491-1.
- Matteucci F and Greggio L (1986), Jan. Relative roles of type I and II supernovae in the chemical enrichment of the interstellar gas. *A&A* 154 (1-2): 279–287.
- Matthee J, Naidu RP, Brammer G, Chisholm J, Eilers AC, Goulding A, Greene J, Kashino D, Labbe I, Lilly SJ, Mackenzie R, Oesch PA, Weibel A, Wuyts S, Xiao M, Bordoloi R, Bouwens R, van Dokkum P, Ilingworth G, Kramarenko I, Maseda MV, Mason C, Meyer RA, Nelson EJ, Reddy NA, Shvaei I, Simcoe RA and Yue M (2024), Mar. Little Red Dots: An Abundant Population of Faint Active Galactic Nuclei at $z \sim 5$ Revealed by the EIGER and FRESCO JWST Surveys. *ApJ* 963 (2), 129. doi:10.3847/1538-4357/ad2345. 2306.05448.
- Mayer L and Bonoli S (2019), Jan. The route to massive black hole formation via merger-driven direct collapse: a review. *Reports on Progress in Physics* 82 (1), 016901. doi:10.1088/1361-6633/aad6a5. 1803.06391.
- McConnell NJ and Ma CP (2013), Feb. Revisiting the Scaling Relations of Black Hole Masses and Host Galaxy Properties. *ApJ* 764 (2), 184. doi:10.1088/0004-637X/764/2/184. 1211.2816.
- McGaugh SS, Schombert JM, Lelli F and Franck J (2024), Nov. Accelerated Structure Formation: The Early Emergence of Massive Galaxies and Clusters of Galaxies. *ApJ* 976 (1), 13. doi:10.3847/1538-4357/ad834d. 2406.17930.
- Menci N, Grazian A, Castellano M, Santini P, Giallongo E, Lamastra A, Fortuni F, Fontana A, Merlin E, Wang T, Elbaz D and Sanchez NG (2020), Sep. Constraints on Dynamical Dark Energy Models from the Abundance of Massive Galaxies at High Redshifts. *ApJ* 900 (2), 108. doi:10.3847/1538-4357/aba9d2. 2007.12453.
- Menci N, Sen AA and Castellano M (2024), Oct. The Excess of JWST Bright Galaxies: a Possible Origin in the Ground State of Dynamical Dark Energy in the light of DESI 2024 Data. *arXiv e-prints*, arXiv:2410.22940doi:10.48550/arXiv.2410.22940. 2410.22940.
- Merlin E, Fortuni F, Torelli M, Santini P, Castellano M, Fontana A, Grazian A, Pentericci L, Pilo S and Schmidt KB (2019), Dec. Red and dead CANDELS: massive passive galaxies at the dawn of the Universe. *MNRAS* 490 (3): 3309–3328. doi:10.1093/mnras/stz2615. 1909.07996.
- Mo HJ and Mao S (2004), Sep. Galaxy formation in pre-processed dark haloes. *MNRAS* 353 (3): 829–840. doi:10.1111/j.1365-2966.2004.08114.x. astro-ph/0311459.
- Mo H, van den Bosch FC and White S (2010). Galaxy Formation and Evolution.
- Mo H, Chen Y and Wang H (2023), Nov. A two-phase model of galaxy formation: I. The growth of galaxies and supermassive black holes. *arXiv e-prints*, arXiv:2311.05030doi:10.48550/arXiv.2311.05030. 2311.05030.
- Moffett AJ, Ingarfield SA, Driver SP, Robotham ASG, Kelvin LS, Lange R, Meštrić U, Alpaslan M, Baldry IK, Bland-Hawthorn J, Brough S, Cluver ME, Davies LJM, Holwerda BW, Hopkins AM, Kafle PR, Kennedy R, Norberg P and Taylor EN (2016a), Apr. Galaxy And Mass Assembly (GAMA): the stellar mass budget by galaxy type. *MNRAS* 457 (2): 1308–1319. doi:10.1093/mnras/stv2883. 1512.02342.
- Moffett AJ, Lange R, Driver SP, Robotham ASG, Kelvin LS, Alpaslan M, Andrews SK, Bland-Hawthorn J, Brough S, Cluver ME, Colless M, Davies LJM, Holwerda BW, Hopkins AM, Kafle PR, Liske J and Meyer M (2016b), Nov. Galaxy and Mass Assembly (GAMA): the stellar mass budget of galaxy spheroids and discs. *MNRAS* 462 (4): 4336–4348. doi:10.1093/mnras/stw1861. 1608.05526.
- Mollá M, Cavichia O, Gavilán M and Gibson BK (2015), Aug. Galactic chemical evolution: stellar yields and the initial mass function. *MNRAS* 451 (4): 3693–3708. doi:10.1093/mnras/stv1102. 1505.03341.
- Monaco P, Fontana F and Taffoni G (2007), Mar. The MORGANA model for the rise of galaxies and active nuclei. *MNRAS* 375 (4): 1189–1219. doi:10.1111/j.1365-2966.2006.11253.x. astro-ph/0610805.
- Moore B, Lake G, Quinn T and Stadel J (1999), Apr. On the survival and destruction of spiral galaxies in clusters. *MNRAS* 304 (3): 465–474. doi:10.1046/j.1365-8711.1999.02345.x. astro-ph/9811127.
- More S, Diemer B and Kravtsov AV (2015), Sep. The Splashback Radius as a Physical Halo Boundary and the Growth of Halo Mass. *ApJ* 810 (1), 36. doi:10.1088/0004-637X/810/1/36. 1504.05591.
- Mortlock DJ, Warren SJ, Venemans BP, Patel M, Hewett PC, McMahon RG, Simpson C, Theuns T, González-Solares EA, Adamson A, Dye S, Hambly NC, Hirst P, Irwin MJ, Kuiper E, Lawrence A and Röttgering HJA (2011), Jun. A luminous quasar at a redshift of $z = 7.085$. *Nature*

- 474 (7353): 616–619. doi:10.1038/nature10159. 1106.6088.
- Moster BP, Somerville RS, Maubetsch C, van den Bosch FC, Macciò AV, Naab T and Oser L (2010), Feb. Constraints on the Relationship between Stellar Mass and Halo Mass at Low and High Redshift. *ApJ* 710 (2): 903–923. doi:10.1088/0004-637X/710/2/903. 0903.4682.
- Moster BP, Naab T and White SDM (2013), Feb. Galactic star formation and accretion histories from matching galaxies to dark matter haloes. *MNRAS* 428 (4): 3121–3138. doi:10.1093/mnras/sts261. 1205.5807.
- Moster BP, Naab T and White SDM (2018), Jun. EMERGE - an empirical model for the formation of galaxies since $z \sim 10$. *MNRAS* 477 (2): 1822–1852. doi:10.1093/mnras/sty655. 1705.05373.
- Naab T and Ostriker JP (2006), Mar. A simple model for the evolution of disc galaxies: the Milky Way. *MNRAS* 366 (3): 899–917. doi:10.1111/j.1365-2966.2005.09807.x. astro-ph/0505594.
- Naab T and Ostriker JP (2017), Aug. Theoretical Challenges in Galaxy Formation. *ARA&A* 55 (1): 59–109. doi:10.1146/annurev-astro-081913-040019. 1612.06891.
- Nanayakkara T, Esdaile J, Glazebrook K, Espejo Salcedo JM, Durre M and Jacobs C (2022), Jan. Massive high-redshift quiescent galaxies with JWST. *PASA* 39, e002. doi:10.1017/pasa.2021.61. 2103.01459.
- Natarajan P (2014), May. Seeds to monsters: tracing the growth of black holes in the universe. *General Relativity and Gravitation* 46, 1702. doi:10.1007/s10714-014-1702-6.
- Navarro JF and Steinmetz M (2000), Aug. Dark Halo and Disk Galaxy Scaling Laws in Hierarchical Universes. *ApJ* 538 (2): 477–488. doi:10.1086/309175. astro-ph/0001003.
- Neal R (2011), MCMC Using Hamiltonian Dynamics, Handbook of Markov Chain Monte Carlo, 113–162.
- Nelson D, Springel V, Pillepich A, Rodriguez-Gomez V, Torrey P, Genel S, Vogelsberger M, Pakmor R, Marinacci F, Weinberger R, Kelley L, Lovell M, Diemer B and Hernquist L (2019), May. The IllustrisTNG simulations: public data release. *Computational Astrophysics and Cosmology* 6 (1), 2. doi:10.1186/s40668-019-0028-x. 1812.05609.
- Pacucci F and Loeb A (2024), Apr. The Redshift Evolution of the $M - M_{\star}$ Relation for JWST's Supermassive Black Holes at $z \lesssim 4$. *ApJ* 964 (2), 154. doi:10.3847/1538-4357/ad3044. 2401.04159.
- Pagel BEJ and Patchett BE (1975), Jul. Metal abundances in nearby stars and the chemical history of the solar neighbourhood. *MNRAS* 172: 13–40. doi:10.1093/mnras/172.1.13.
- Pandya V, Fielding DB, Anglés-Alcázar D, Somerville RS, Bryan GL, Hayward CC, Stern J, Kim CG, Quataert E, Forbes JC, Faucher-Giguère CA, Feldmann R, Hafen Z, Hopkins PF, Kereš D, Murray N and Weizel A (2021), Dec. Characterizing mass, momentum, energy, and metal outflow rates of multiphase galactic winds in the FIRE-2 cosmological simulations. *MNRAS* 508 (2): 2979–3008. doi:10.1093/mnras/stab2714. 2103.06891.
- Pantoni L, Lapi A, Massardi M, Goswami S and Danese L (2019), Aug. New Analytic Solutions for Galaxy Evolution: Gas, Stars, Metals, and Dust in Local ETGs and Their High- z Star-forming Progenitors. *ApJ* 880 (2), 129. doi:10.3847/1538-4357/ab2adc. 1906.07458.
- Pezzulli G and Fraternali F (2016), Jan. Accretion, radial flows and abundance gradients in spiral galaxies. *MNRAS* 455 (3): 2308–2322. doi:10.1093/mnras/stv2397. 1510.04289.
- Pillepich A, Springel V, Nelson D, Genel S, Naiman J, Pakmor R, Hernquist L, Torrey P, Vogelsberger M, Weinberger R and Marinacci F (2018), Jan. Simulating galaxy formation with the IllustrisTNG model. *MNRAS* 473 (3): 4077–4106. doi:10.1093/mnras/stx2656. 1703.02970.
- Pillepich A, Nelson D, Springel V, Pakmor R, Torrey P, Weinberger R, Vogelsberger M, Marinacci F, Genel S, van der Wel A and Hernquist L (2019), Dec. First results from the TNG50 simulation: the evolution of stellar and gaseous discs across cosmic time. *MNRAS* 490 (3): 3196–3233. doi:10.1093/mnras/stz2338. 1902.05553.
- Pipino A, Lilly SJ and Carollo CM (2014), Jun. On the relation between specific star formation rate and metallicity. *MNRAS* 441 (2): 1444–1456. doi:10.1093/mnras/stu579. 1403.6146.
- Popesso P, Concas A, Cresci G, Belli S, Rodighiero G, Inami H, Dickinson M, Ilbert O, Pannella M and Elbaz D (2023), Feb. The main sequence of star-forming galaxies across cosmic times. *MNRAS* 519 (1): 1526–1544. doi:10.1093/mnras/stac3214. 2203.10487.
- Recchi S, Spitoni E, Matteucci F and Lanfranchi GA (2008), Oct. The effect of differential galactic winds on the chemical evolution of galaxies. *A&A* 489 (2): 555–565. doi:10.1051/0004-6361:200809879. 0808.0118.
- Recchi S, Kroupa P and Ploekinger S (2015), Jul. The mass-metallicity relation of tidal dwarf galaxies. *MNRAS* 450 (3): 2367–2372. doi:10.1093/mnras/stv798. 1504.02473.
- Reed SL, Banerji M, Becker GD, Hewett PC, Martini P, McMahon RG, Pons E, Rauch M, Abbott TMC, Allam S, Annis J, Avila S, Bertin E, Brooks D, Buckley-Geer E, Carrero Rosell A, Carrasco Kind M, Carretero J, Castander FJ, Cunha CE, D'Andrea CB, da Costa LN, De Vicente J, Desai S, Diehl HT, Doel P, Evrard AE, Flaugher B, Frieman J, García-Bellido J, Gaztanaga E, Gruen D, Gschwend J, Gutierrez G, Hollowood DL, Honscheid K, Hoyle B, James DJ, Kuehn K, Lahav O, Lima M, Maia MAG, Marshall JL, Miquel R, Ogando RLC, Plazas AA, Roodman A, Sanchez E, Scarpine V, Schubnell M, Serrano S, Sevilla-Noarbe I, Smith M, Smith RC, Sobreira F, Suchyta E, Swanson MEC, Tarle G, Thomas D, Tucker DL and Vikram V (2019), Aug. Three new VHS-DES quasars at $6.7 \lesssim z \lesssim 6.9$ and emission line properties at $z \lesssim 6.5$. *MNRAS* 487 (2): 1874–1885. doi:10.1093/mnras/stz1341. 1901.07456.
- Reines AE and Volonteri M (2015), Nov. Relations between Central Black Hole Mass and Total Galaxy Stellar Mass in the Local Universe. *ApJ* 813 (2), 82. doi:10.1088/0004-637X/813/2/82. 1508.06274.
- Reyes R, Mandelbaum R, Gunn JE, Nakajima R, Seljak U and Hirata CM (2012), Oct. Optical-to-virial velocity ratios of local disc galaxies from combined kinematics and galaxy-galaxy lensing. *MNRAS* 425 (4): 2610–2640. doi:10.1111/j.1365-2966.2012.21472.x. 1110.4107.
- Rodighiero G, Daddi E, Baronchelli I, Cimatti A, Renzini A, Aussel H, Popesso P, Lutz D, Andreani P, Berta S, Cava A, Elbaz D, Feltre A, Fontana A, Förster Schreiber NM, Franceschini A, Genzel R, Grazian A, Gruppioni C, Ilbert O, Le Floch E, Magdis G, Magliocchetti M, Magnelli B, Maiolino R, McCracken H, Nordon R, Poglitsch A, Santini P, Pozzi F, Riguccini L, Tacconi LJ, Wuyts S and Zamorani G (2011), Oct. The Lesser Role of Starbursts in Star Formation at $z = 2$. *ApJ* 739 (2), L40. doi:10.1088/2041-8205/739/2/L40. 1108.0933.
- Rodighiero G, Brusa M, Daddi E, Negrello M, Mullaney JR, Delvecchio I, Lutz D, Renzini A, Franceschini A, Baronchelli I, Pozzi F, Gruppioni C, Strazzullo V, Cimatti A and Silverman J (2015), Feb. Relationship between Star Formation Rate and Black Hole Accretion At $Z = 2$: the Different Contributions in Quiescent, Normal, and Starburst Galaxies. *ApJ* 800 (1), L10. doi:10.1088/2041-8205/800/1/L10. 1501.04634.
- Rodríguez-Puebla A, Primack JR, Avila-Reese V and Faber SM (2017), Sep. Constraining the galaxy-halo connection over the last 13.3 Gyr: star formation histories, galaxy mergers and structural properties. *MNRAS* 470 (1): 651–687. doi:10.1093/mnras/stx1172. 1703.04542.
- Roediger E, Bruggen M, Owers MS, Ebeling H and Sun M (2014), Sep. Star formation in shocked cluster spirals and their tails. *MNRAS* 443: L114–L118. doi:10.1093/mnras/lsu087. 1405.1033.
- Roy A and Lapi A (2024), Jul. Semi-Empirical Approach to [CII] Line Intensity Mapping. *arXiv e-prints*, arXiv:2407.19007doi:10.48550/arXiv.2407.19007. 2407.19007.
- Sahu N, Graham AW and Davis BL (2019), May. Black Hole Mass Scaling Relations for Early-type Galaxies. I. $M_{BH} - M_{\star, sph}$ and $M_{BH} - M_{\star, gal}$. *ApJ* 876 (2), 155. doi:10.3847/1538-4357/ab0f32. 1903.04738.
- Sargent MT, Béthermin M, Daddi E and Elbaz D (2012), Mar. The Contribution of Starbursts and Normal Galaxies to Infrared Luminosity

- Functions at $z \leq 2$. *ApJ* 747 (2), L31. doi:10.1088/2041-8205/747/2/L31. 1202.0290.
- Scannapieco C, Tissera PB, White SDM and Springel V (2008), Sep. Effects of supernova feedback on the formation of galaxy discs. *MNRAS* 389 (3): 1137–1149. doi:10.1111/j.1365-2966.2008.13678.x. 0804.3795.
- Scannapieco C, Wadepuhl M, Parry OH, Navarro JF, Jenkins A, Springel V, Teyssier R, Carlson E, Couchman HMP, Crain RA, Dalla Vecchia C, Frenk CS, Kobayashi C, Monaco P, Murante G, Okamoto T, Quinn T, Schaye J, Stinson GS, Theuns T, Wadsley J, White SDM and Woods R (2012), Jun. The Aquila comparison project: the effects of feedback and numerical methods on simulations of galaxy formation. *MNRAS* 423 (2): 1726–1749. doi:10.1111/j.1365-2966.2012.20993.x. 1112.0315.
- Schaye J, Crain RA, Bower RG, Furlong M, Schaller M, Theuns T, Dalla Vecchia C, Frenk CS, McCarthy IG, Helly JC, Jenkins A, Rosas-Guevara YM, White SDM, Baes M, Booth CM, Camps P, Navarro JF, Qu Y, Rahmati A, Sawala T, Thomas PA and Trayford J (2015), Jan. The EAGLE project: simulating the evolution and assembly of galaxies and their environments. *MNRAS* 446 (1): 521–554. doi:10.1093/mnras/stu2058. 1407.7040.
- Schmidt M (1963), Apr. The Rate of Star Formation. II. The Rate of Formation of Stars of Different Mass. *ApJ* 137: 758. doi:10.1086/147553.
- Schreiber C, Pannella M, Elbaz D, Béthermin M, Inami H, Dickinson M, Magnelli B, Wang T, Aussel H, Daddi E, Juneau S, Shu X, Sargent MT, Buat V, Faber SM, Ferguson HC, Giavalisco M, Koekemoer AM, Magdis G, Morrison GE, Papovich C, Santini P and Scott D (2015), Mar. The Herschel view of the dominant mode of galaxy growth from $z = 4$ to the present day. *A&A* 575, A74. doi:10.1051/0004-6361/201425017. 1409.5433.
- Shakura NI and Sunyaev RA (1973), Jan. Black holes in binary systems. Observational appearance. *A&A* 24: 337–355.
- Shandarin S, Habib S and Heitmann K (2012), Apr. Cosmic web, multistream flows, and tessellations. *PRD* 85 (8), 083005. doi:10.1103/PhysRevD.85.083005. 1111.2366.
- Shankar F, Lapi A, Salucci P, De Zotti G and Danese L (2006), May. New Relationships between Galaxy Properties and Host Halo Mass, and the Role of Feedbacks in Galaxy Formation. *ApJ* 643 (1): 14–25. doi:10.1086/502794. astro-ph/0601577.
- Shankar F, Guo H, Bouillot V, Rettura A, Meert A, Buchan S, Kravtsov A, Bernardi M, Sheth R, Vikram V, Marchesini D, Behroozi P, Zheng Z, Maraston C, Ascaso B, Lemaux BC, Capozzi D, Huertas-Company M, Gal RR, Lubin LM, Conselice CJ, Carollo M and Cattaneo A (2014), Dec. On the Intermediate-redshift Central Stellar Mass-Halo Mass Relation, and Implications for the Evolution of the Most Massive Galaxies Since $z \sim 1$. *ApJ* 797 (2), L27. doi:10.1088/2041-8205/797/2/L27. 1411.2597.
- Shankar F, Bernardi M, Sheth RK, Ferrarese L, Graham AW, Savorgnan G, Allevato V, Marconi A, Läscher R and Lapi A (2016), Aug. Selection bias in dynamically measured supermassive black hole samples: its consequences and the quest for the most fundamental relation. *MNRAS* 460 (3): 3119–3142. doi:10.1093/mnras/stw678. 1603.01276.
- Silk J and Mamon GA (2012), Aug. The current status of galaxy formation. *Research in Astronomy and Astrophysics* 12 (8): 917–946. doi:10.1088/1674-4527/12/8/004. 1207.3080.
- Silk J and Rees MJ (1998), Mar. Quasars and galaxy formation. *A&A* 331: L1–L4. doi:10.48550/arXiv.astro-ph/9801013. astro-ph/9801013.
- Skilling J (2004), Nov., Nested Sampling, Fischer R, Preuss R and Toussaint UV, (Eds.), Bayesian Inference and Maximum Entropy Methods in Science and Engineering: 24th International Workshop on Bayesian Inference and Maximum Entropy Methods in Science and Engineering, American Institute of Physics Conference Series, 735, AIP, 395–405.
- Somerville RS and Davé R (2015), Aug. Physical Models of Galaxy Formation in a Cosmological Framework. *ARA&A* 53: 51–113. doi:10.1146/annurev-astro-082812-140951. 1412.2712.
- Somerville RS, Hopkins PF, Cox TJ, Robertson BE and Hernquist L (2008), Dec. A semi-analytic model for the co-evolution of galaxies, black holes and active galactic nuclei. *MNRAS* 391 (2): 481–506. doi:10.1111/j.1365-2966.2008.13805.x. 0808.1227.
- Somerville RS, Gilmore RC, Primack JR and Domínguez A (2012), Jul. Galaxy properties from the ultraviolet to the far-infrared: Λ cold dark matter models confront observations. *MNRAS* 423 (3): 1992–2015. doi:10.1111/j.1365-2966.2012.20490.x. 1104.0669.
- Somerville RS, Popping G and Trager SC (2015), Nov. Star formation in semi-analytic galaxy formation models with multiphase gas. *MNRAS* 453 (4): 4337–4367. doi:10.1093/mnras/stv1877. 1503.00755.
- Speagle JS, Steinhardt CL, Capak PL and Silverman JD (2014), Oct. A Highly Consistent Framework for the Evolution of the Star-Forming “Main Sequence” from $z \sim 0$ –6. *ApJS* 214 (2), 15. doi:10.1088/0067-0049/214/2/15. 1405.2041.
- Spitoni E, Vincenzo F and Matteucci F (2017), Mar. New analytical solutions for chemical evolution models: characterizing the population of star-forming and passive galaxies. *A&A* 599, A6. doi:10.1051/0004-6361/201629745. 1605.05603.
- Springel V, Frenk CS and White SDM (2006), Apr. The large-scale structure of the Universe. *Nature* 440 (7088): 1137–1144. doi:10.1038/nature04805. astro-ph/0604561.
- Steinhauser D, Schindler S and Springel V (2016), Jun. Simulations of ram-pressure stripping in galaxy-cluster interactions. *A&A* 591, A51. doi:10.1051/0004-6361/201527705. 1604.05193.
- Stevens ARH, Croton DJ and Mutch SJ (2016), Sep. Building disc structure and galaxy properties through angular momentum: the DARK SAGE semi-analytic model. *MNRAS* 461 (1): 859–876. doi:10.1093/mnras/stw1332. 1605.00647.
- Stinson GS, Brook C, Macciò AV, Wadsley J, Quinn TR and Couchman HMP (2013), Jan. Making Galaxies In a Cosmological Context: the need for early stellar feedback. *MNRAS* 428 (1): 129–140. doi:10.1093/mnras/sts028. 1208.0002.
- Stone MA, Lyu J, Rieke GH, Alberts S and Hainline KN (2024), Mar. Undermassive Host Galaxies of Five $z \sim 6$ Luminous Quasars Detected with JWST. *ApJ* 964 (1), 90. doi:10.3847/1538-4357/ad2a57. 2310.18395.
- Talbot Raymond J. J and Arnett WD (1971), Dec. The Evolution of Galaxies. I. Formulation and Mathematical Behavior of the One-Zone Model. *ApJ* 170: 409. doi:10.1086/151228.
- Thomas D, Maraston C and Bender R (2005), Jan., The Epochs of Early-Type Galaxy Formation in Clusters and in the Field, Renzini A and Bender R, (Eds.), Multiwavelength Mapping of Galaxy Formation and Evolution, pp. 296.
- Thomas D, Maraston C, Schawinski K, Sarzi M and Silk J (2010), Jun. Environment and self-regulation in galaxy formation. *MNRAS* 404 (4): 1775–1789. doi:10.1111/j.1365-2966.2010.16427.x. 0912.0259.
- Tinker J, Kravtsov AV, Klypin A, Abazajian K, Warren M, Yepes G, Gottlöber S and Holz DE (2008), Dec. Toward a Halo Mass Function for Precision Cosmology: The Limits of Universality. *ApJ* 688 (2): 709–728. doi:10.1086/591439. 0803.2706.
- Tinsley BM (1974), Sep. Constraints on models for chemical evolution in the solar neighborhood. *ApJ* 192: 629–641. doi:10.1086/153099.
- Tinsley BM (1980), Jan. Evolution of the Stars and Gas in Galaxies. *FChP* 5: 287–388. doi:10.48550/arXiv.2203.02041. 2203.02041.
- Tollet É, Cattaneo A, Mamon GA, Moutard T and van den Bosch FC (2017), Nov. On stellar mass loss from galaxies in groups and clusters. *MNRAS* 471 (4): 4170–4193. doi:10.1093/mnras/stx1840. 1707.06264.
- Tomczak AR, Quadri RF, Tran KVH, Labbé I, Straatman CMS, Papovich C, Glazebrook K, Allen R, Brammer GB, Kacprzak GG, Kawinwanichakij L, Kelson DD, McCarthy PJ, Mehrrens N, Monson AJ, Persson SE, Spitler LR, Tilvi V and van Dokkum P (2014), Mar. Galaxy Stellar Mass Functions from ZFOURGE/CANDELS: An Excess of Low-mass Galaxies since $z = 2$ and the Rapid Buildup of Quiescent Galaxies. *ApJ* 783 (2), 85. doi:10.1088/0004-637X/783/2/85. 1309.5972.
- Tremaine S, Gebhardt K, Bender R, Bower G, Dressler A, Faber SM, Filippenko AV, Green R, Grillmair C, Ho LC, Kormendy J, Lauer TR,

- Magorrian J, Pinkney J and Richstone D (2002), Aug. The Slope of the Black Hole Mass versus Velocity Dispersion Correlation. *ApJ* 574 (2): 740–753. doi:10.1086/341002. astro-ph/0203468.
- Übler H, Maiolino R, Curtis-Lake E, Pérez-González PG, Curti M, Perna M, Arribas S, Charlot S, Marshall MA, D'Eugenio F, Scholtz J, Bunker A, Carniani S, Ferruit P, Jakobsen P, Rix HW, Rodríguez Del Pino B, Willott CJ, Boeker T, Cresci G, Jones GC, Kumari N and Rawle T (2023), Sep. GA-NIFS: A massive black hole in a low-metallicity AGN at $z \sim 5.55$ revealed by JWST/NIRSpec IFS. *A&A* 677, A145. doi: 10.1051/0004-6361/202346137. 2302.06647.
- Vale A and Ostriker JP (2004), Sep. Linking halo mass to galaxy luminosity. *MNRAS* 353 (1): 189–200. doi:10.1111/j.1365-2966.2004.08059.x. astro-ph/0402500.
- Vale A and Ostriker JP (2006), Sep. The non-parametric model for linking galaxy luminosity with halo/subhalo mass. *MNRAS* 371 (3): 1173–1187. doi:10.1111/j.1365-2966.2006.10605.x. astro-ph/0511816.
- Valentini M, Murante G, Borgani S, Granato GL, Monaco P, Brighenti F, Tornatore L, Bressan A and Lapi A (2020), Jan. Impact of AGN feedback on galaxies and their multiphase ISM across cosmic time. *MNRAS* 491 (2): 2779–2807. doi:10.1093/mnras/stz3131. 1911.02572.
- Vincenzo F, Kobayashi C and Yuan T (2019), Oct. Zoom-in cosmological hydrodynamical simulation of a star-forming barred, spiral galaxy at redshift $z = 2$. *MNRAS* 488 (4): 4674–4689. doi:10.1093/mnras/stz2065. 1903.07958.
- Vogelsberger M, Genel S, Springel V, Torrey P, Sijacki D, Xu D, Snyder G, Bird S, Nelson D and Hernquist L (2014), May. Properties of galaxies reproduced by a hydrodynamic simulation. *Nature* 509 (7499): 177–182. doi:10.1038/nature13316. 1405.1418.
- Volonteri M, Habouzit M and Colpi M (2021), Sep. The origins of massive black holes. *Nature Reviews Physics* 3 (11): 732–743. doi:10.1038/s42254-021-00364-9. 2110.10175.
- Wang F, Wu XB, Fan X, Yang J, Cai Z, Yi W, Zuo W, Wang R, McGreer ID, Ho LC, Kim M, Yang Q, Bian F and Jiang L (2015), Jul. An Ultra-luminous Quasar at $z = 5.363$ with a Ten Billion Solar Mass Black Hole and a Metal-rich DLA at $z \sim 5$. *ApJ* 807 (1), L9. doi:10.1088/2041-8205/807/1/L9. 1506.01765.
- Wang F, Yang J, Fan X, Yue M, Wu XB, Schindler JT, Bian F, Li JT, Farina EP, Bañados E, Davies FB, Decarli R, Green R, Jiang L, Hennawi JF, Huang YH, Mazzucchelli C, McGreer ID, Venemans B, Walter F and Beletsky Y (2018), Dec. The Discovery of a Luminous Broad Absorption Line Quasar at a Redshift of 7.02. *ApJ* 869 (1), L9. doi:10.3847/2041-8213/aaf1d2. 1810.11925.
- Weaver JR, Davidzon I, Toft S, Ilbert O, McCracken HJ, Gould KML, Jespersen CK, Steinhardt C, Lagos CDP, Capak PL, Casey CM, Chartab N, Faisst AL, Hayward CC, Kartaltepe JS, Kauffmann OB, Koekemoer AM, Kokorev V, Laigle C, Liu D, Long A, Magdis GE, McPartland CJR, Milvang-Jensen B, Mobasher B, Moneti A, Peng Y, Sanders DB, Shuntov M, Sneppen A, Valentino F, Zalesky L and Zamorani G (2023), Sep. COSMOS2020: The galaxy stellar mass function. The assembly and star formation cessation of galaxies at $0.2 < z \leq 7.5$. *A&A* 677, A184. doi:10.1051/0004-6361/202245581. 2212.02512.
- Wechsler RH, Bullock JS, Primack JR, Kravtsov AV and Dekel A (2002), Mar. Concentrations of Dark Halos from Their Assembly Histories. *ApJ* 568 (1): 52–70. doi:10.1086/338765. astro-ph/0108151.
- Wellons S, Faucher-Giguère CA, Hopkins PF, Quataert E, Anglés-Alcázar D, Feldmann R, Hayward CC, Kereš D, Su KY and Wetzel A (2023), Apr. Exploring supermassive black hole physics and galaxy quenching across halo mass in FIRE cosmological zoom simulations. *MNRAS* 520 (4): 5394–5412. doi:10.1093/mnras/stad511. 2203.06201.
- Whitaker KE, Franx M, Leja J, van Dokkum PG, Henry A, Skelton RE, Fumagalli M, Momcheva IG, Brammer GB, Labbé I, Nelson EJ and Rigby JR (2014), Nov. Constraining the Low-mass Slope of the Star Formation Sequence at $0.5 < z < 2.5$. *ApJ* 795 (2), 104. doi:10.1088/0004-637X/795/2/104. 1407.1843.
- Wilding G, Nevenzeel K, van de Weygaert R, Vegter G, Pranav P, Jones BJT, Efstathiou K and Feldbrugge J (2021), Oct. Persistent homology of the cosmic web - I. Hierarchical topology in Λ CDM cosmologies. *MNRAS* 507 (2): 2968–2990. doi:10.1093/mnras/stab2326. 2011.12851.
- Wuyts S, Förster Schreiber NM, van der Wel A, Magnelli B, Guo Y, Genzel R, Lutz D, Aussel H, Barro G, Berta S, Cava A, Graciá-Carpio J, Hathi NP, Huang KH, Kocevski DD, Koekemoer AM, Lee KS, Le Floch E, McGrath EJ, Nordon R, Popesso P, Pozzi F, Riguccini L, Rodighiero G, Saintonge A and Tacconi L (2011), Dec. Galaxy Structure and Mode of Star Formation in the SFR-Mass Plane from $z = -2.5$ to $z = 0.1$. *ApJ* 742 (2), 96. doi:10.1088/0004-637X/742/2/96. 1107.0317.
- Yang X, Mo HJ, van den Bosch FC, Zhang Y and Han J (2012), Jun. Evolution of the Galaxy-Dark Matter Connection and the Assembly of Galaxies in Dark Matter Halos. *ApJ* 752 (1), 41. doi:10.1088/0004-637X/752/1/41. 1110.1420.
- Yang J, Wang F, Fan X, Barth AJ, Hennawi JF, Nanni R, Bian F, Davies FB, Farina EP, Schindler JT, Bañados E, Decarli R, Eilers AC, Green R, Guo H, Jiang L, Li JT, Venemans B, Walter F, Wu XB and Yue M (2021a), Dec. Probing Early Supermassive Black Hole Growth and Quasar Evolution with Near-infrared Spectroscopy of 37 Reionization-era Quasars at $6.3 < z \leq 7.64$. *ApJ* 923 (2), 262. doi:10.3847/1538-4357/ac2b32. 2109.13942.
- Yang J, Wang F, Fan X, Barth AJ, Hennawi JF, Nanni R, Bian F, Davies FB, Farina EP, Schindler JT, Bañados E, Decarli R, Eilers AC, Green R, Guo H, Jiang L, Li JT, Venemans B, Walter F, Wu XB and Yue M (2021b), Dec. Probing Early Supermassive Black Hole Growth and Quasar Evolution with Near-infrared Spectroscopy of 37 Reionization-era Quasars at $6.3 < z \leq 7.64$. *ApJ* 923 (2), 262. doi:10.3847/1538-4357/ac2b32. 2109.13942.
- Yue M, Eilers AC, Ananna TT, Panagiotou C, Kara E and Miyaji T (2024), Apr. Stacking X-ray Observations of “Little Red Dots”: Implications for their AGN Properties. *arXiv e-prints*, arXiv:2404.13290doi:10.48550/arXiv.2404.13290. 2404.13290.
- Zavala J, Avila-Reese V, Firmani C and Boylan-Kolchin M (2012), Dec. The growth of galactic bulges through mergers in Λ CDM haloes revisited - I. Present-day properties. *MNRAS* 427 (2): 1503–1516. doi:10.1111/j.1365-2966.2012.22100.x. 1204.0516.
- Zemp M (2014), Sep. On Physical Scales of Dark Matter Halos. *ApJ* 792 (2), 124. doi:10.1088/0004-637X/792/2/124. 1312.4629.
- Zhang H, Behroozi P, Volonteri M, Silk J, Fan X, Hopkins PF, Yang J and Aird J (2023), Jan. TRINITY I: self-consistently modelling the dark matter halo-galaxy-supermassive black hole connection from $z = 0-10$. *MNRAS* 518 (2): 2123–2163. doi:10.1093/mnras/stac2633. 2105.10474.
- Zhang H, Behroozi P, Volonteri M, Silk J, Fan X, Aird J, Yang J and Hopkins PF (2024a), Apr. TRINITY - III. Quasar luminosity functions decomposed by halo, galaxy, and black hole masses as well as Eddington ratios from $z = 0-10$. *MNRAS* 529 (3): 2777–2793. doi:10.1093/mnras/stae655. 2305.19315.
- Zhang X, Lachance P, Ni Y, Li Y, Croft RAC, Matteo TD, Bird S and Feng Y (2024b), Feb. AI-assisted super-resolution cosmological simulations III: time evolution. *MNRAS* 528 (1): 281–293. doi:10.1093/mnras/stad3940. 2305.12222.
- Zhao DH, Mo HJ, Jing YP and Börner G (2003), Feb. The growth and structure of dark matter haloes. *MNRAS* 339 (1): 12–24. doi:10.1046/j.1365-8711.2003.06135.x. astro-ph/0204108.
- Zhao DH, Jing YP, Mo HJ and Börner G (2009), Dec. Accurate Universal Models for the Mass Accretion Histories and Concentrations of Dark Matter Halos. *ApJ* 707 (1): 354–369. doi:10.1088/0004-637X/707/1/354. 0811.0828.
- Zhu P, Ho LC and Gao H (2021), Jan. The Correlation between Black Hole Mass and Stellar Mass for Classical Bulges and the Cores of Ellipticals. *ApJ* 907 (1), 6. doi:10.3847/1538-4357/abcaa1. 2011.07216.
- Zhukovska S, Gail HP and Trieloff M (2008), Feb. Evolution of interstellar dust and stardust in the solar neighbourhood. *A&A* 479 (2): 453–480. doi:10.1051/0004-6361:20077789. 0706.1155.